KINETICS OF OIL DISPERSION IN THE PRESENCE OF CHITOSAN BASED BIOPOLYMERS

A Thesis Submitted to
the Graduate School of Engineering and Sciences of
İzmir Institute of Technology
in Partial Fulfillment of the Requirements for the Degree of

MASTER OF SCIENCE

in Chemistry

by
Didem ŞEN

December 2009
İZMİR

We approve the thesis of **Didem ŞEN**

Prof. Dr. Hürriyet POLAT
Supervisor

Prof.Dr. Devrim BALKÖSE
Committee Member

Assoc.Prof. Dr. Mustafa DEMİR
Committee Member

16 December 2009

Prof.Dr. Levent ARTOK
Head of the Department of Chemistry

Assoc.Prof.Dr. Talat YALÇIN
Dean of the Graduate School of Engineering and Sciences

ACKNOWLEDGEMENTS

I would like to thank the people who have assisted me in preparing this thesis.First Iwould like to express my grateful thanks to my supervisor Prof.Dr. Hürriyet POLAT for her guidance, motivation and endless supports during this thesis. Also I am grateful to Prof.Dr. Mehmet POLAT, Prof.Dr. Ahmet Emin EROĞLU , all my committee members and Serkan KELEŞOĞLU for their valuable comments during the experimental period.

I am also thankful to assistance of The Center of Material Research, The Center of Biotechnology and Bioengineering Research and Dr.Hüseyin ÖZGENER during experimental period.

Special thanks to all Research Assistants in Chemistry Department for their helps and friendships.

Additionally, I would like to express my gratefulness to Dr. Betül ÖZTÜRK, Research Assistant İbrahim KARAMAN and my dear friend Ayşegül YALÇIN for their encouragement, friendship over two years period of my academic life.

I would like to thank my family for their endless support, continued patience and encouragement throughout my education.

Finally, I want to express my appreciation to my beloved Sergeant İbrahim KARAMAN whose dedication, love and confidence in me have taken load off my shoulder. I owe him so much.

ABSTRACT

KINETICS OF OIL DISPERSION IN THE PRESENCE OF CHITOSAN BASED BIOPOLYMERS

This study was focused on the modification of chitosan to produce surface active biopolymers and their application as emulsifiers. Therefore N-acylation of chitosan was utilized. Characterization of the produced materials were achieved by the following ways; Ninhydrin assay, Elemental Analysis, Fourier Transform Infrared Spektroscopy (FTIR), X-Ray Diffraction (XRD), Scanning Electron Microscope (SEM), surface (or interfacial) tension and contact angle measurements. These characterizations provided information about the substitution degree, structure and the hydrophobic-hydrophilic properties of the produced surface active biopolymer. For example, the surface tension values were determined as decreasing from 71 mN/m to 40-50 mN/m in the presence of chitosan based bio-polymers with the substitution degrees between 25% and 45%. On the other hand contact angle values increased significantly in the case of chitosan based biopolymers' modifications with different initial mol ratios.

The effect of these modified materials on the kinetics of oil emulsification was tested conducting in-situ size measurement studies and using a phenomenological dispersion model for the evaluation of data. This way the dispersion rate constants were able to calculated and used to compare the different conditions used to prepare emulsions. As a conclusion, the coalescence sub process that becomes dominant after 8 minutes of emulsification (in the case of oil only) totally disappeared in the presence of both chitosan and N-acylated chitosan. The rate of oil dispersion up to 8 minutes, however, did not change much in all the cases. The effect of modified chitosan on the kinetics was not significant. These were postulated as the possible changes in the configurations of the modified chitosan molecules due to the increased hydrophobic character and inter molecule interactions.

ÖZET

KİTOSAN BAZLI BİYOPOLYMERLER VARLIĞINDA YAĞ DAĞILIM KİNETİĞİ

Bu çalışma yüzey aktif biyopolimerler üretmek için kitosanın modifiye edilmesine ve bunların emülsifiyer olarak kullanımasına odaklanmıştır. Bu sebeple kitosana N-açilleme uygulanmıştır.Üretilen bu malzemelerin karakterizasyonu şu yöntemlerle gerçekleştirilmiştir; Ninhydrin testi, Elemental analiz, Fourier dönüşümlü infrared spektroskopi (FTIR), Taramalı electron mikroskobu (SEM), yüzey (yada arayüzey) gerilimi ve kontak açısı ölçümü. Bu karakterize etme yöntemleri üretilen yüzey aktif biyopolimerin yer değiştirme yüzdesi, yapısı ve sudan korkma -suyu sevme özellikleri hakkında bilgi sağlamıştır. Örneğin; yüzey gerilimi %25 ile %45 yer değişimi sağlanmış kitosan bazlı yüzey aktif maddeler varlığında 71 mN/m den 40-50 mN/m e düşmüştür. Kontak açısı değerleri ise farklı başlangıç mol oralarına sahip kitosan bazlı yüzey aktif maddeler varlığında önemli oranda yükselmiştir.

Modifiye edilmiş bu malzemelerin yağ emülsiyonu üzerindeki etkisi in-situ boyut ölçümü ve bu ölçümlerin verilerine uygulanan fenomenoljik dağılım modeli ile test edilmiştir. Bu yol ile farklı koşullarda hazırlanmış emülsiyonların dağılım hızlarının hesaplanması ve bu hızların karşılaştırması sağlanmıştır. Sonuç olarak ; sadece yağın bulunduğu durumda 8 dakikadan sonra baskın hale gelen birleşme alt işlemi kitosan ve N-açillenmiş kitosan varlığında tamamen kaybolmuştur. Fakat kitosan ve N-açillenmiş kitosan varlığında olan durumlarda da 8 dakikaya kadar olan yağ dağılım hızı fazla değişiklik göstermemiştir. Ayrıca N-açillenmiş kitosanın yağ dağılım kinetiğine olan etkisinin önemli miktarda olmadığı gözlemlenmiştir. Tüm bunların modifiye edilmiş kitosanın olası konfigürasyon değişiklerinden ve molekül içindeki etkileşimlerden dolayı olduğu kabul edilmiştir.

TABLE OF CONTENTS

LIST OF FIGURES

LIST OF TABLES

CHAPTER 1

INTRODUCTION

1.1. Consideration on Dispersions

Dispersions are the systems that contain slightly soluble or insoluble distributed particles in a continuous phase. The distributed particles in a continuous phase form the dispersed phase .The dispersed and continuous phases may be a solid, a liquid or a gas. (Table 1.1. Dispersion Systems) (Kissa 1999).

Table 1.1. Dispersion Systems
(Kissa E. 1999)

Continuous Phase	Dispersed Phase	Description
Gas	Liquid	Mist
Gas	Solid	Smoke
Liquid	Gas	Foam
Liquid	Liquid	Emulsion
Liquid	Solid	Suspension
Solid	Gas	Solid Foam
Solid	Liquid	Solid emulsion
Solid	Solid	Solid Suspension

1.2. Statement of Oil Dispersion Problems

Many industrial applications include dispersions of solid/liquid (suspension) and liquid/liquid (emulsions) types (Tadros, et al. 2004). Especially oil in water or water in oil dispersed systems are pertained to daily life and industry because of their widespread existence in many applications. These systems are prevalently known as emulsions. Emulsions can take place from material processing of metal working and textile to cosmetic, pharmaceutical and food products (Abismaïl 2000).

Due to emulsions have this much application areas, encountered problems during processing also increase. When pure oil and water are placed in a container these two immiscible liquids break in two separate phases with time. Emulsified systems' this thermodynamically unstable characteristic cause financial loses especially in the industrial applications. For this reason, in all application areas resistance to phase separation and having knowledge about the characteristic properties of emulsions which in turn determine the success of emulsions gain importance.

The stability in emulsion system might be expressed as the invariability of number of particles per medium volume during storage time. Therefore prediction and control of size distribution of dispersed oil droplets are important for emulsions. In the following parts some methods that are used to evaluate particle shapes, size and size distributions of dispersed systems will be briefly summarized.

1.3. Common Ways to Provide Oil Dispersion in Water

The mechanical energy that is applied during oil in water dispersion is known as homogenization. The homogenization is a physical process which is used to intermingle the oil and water phases and form oil droplets if the emulsion is considered as O/W emulsion. During the homogenization the oil droplets tend to form large droplets by coalescing with neighboring droplets. To prevent the coalescence and provide kinetic stability sufficient concentration of emulsifier should be present while the homogenization is applied (MCClement 2005, Leal-Calderon, et al. 2007).

Different homogenization methods have been developed according to the volume of starting material, the desired droplet size distribution, the required physicochemical properties of the final product developed to be applied in suitable emulsification processes. These processes are, High Pressure Homogenization, Ultrasonic Jet Homogenization, Microfludization, Membrane and Microchannel Homogenization. Through the following chapters some important homogenization routes and types of emulsifiers that are widely used will be briefly summarized.

Utilization of emulsifiers is one of the most widely used methods to improve the stability of oil-in water emulsions. These materials are surface-active ingredients that adsorb at the interfaces and improve the long term stability of emulsions (Polat, et al. 1999).

Emulsifiers can be categorized into two groups; synthetic and natural emulsifiers. This will be subject of Chapter 2 (Egger and McGrath 2006).

Among various macromolecules proteins and polysaccharides are often used in the food, pharmaceutical, and cosmetic industries. Chitosan is one of these materials which have an increase in use.

Chitosan (N-deacetylated-2-acetamido-2-deoxy-β-D-glucan) is a unique cationic polysaccharide and in the literature takes place as a useful emulsifier which has biodegradable, biocompatible properties. Most commercial polysaccharides (e.g. cellulose, alginic acid, pectin, gum arabic, and dextran) are either neutral or anionic but chitosan is cationic. This positively charged chitosan is obtained when chitosan is dissolved in dilute acid and was observed to have influence on flocculation process, film forming. Also chitosan has been used as emulsifying, thickening and stabilizing agent (Kumar-Anal, et al. 2008).Chitosan was suggested to combine both viscosifying and electrosteric stabilization in literature (Rodriguez, et al. 2002). The electrosteric stabilization is defined as the combination of steric stabilization and electrostatic stabilization.

Chitosan derivatives were also used in emulsion systems such as hydrophobically modified chitosan derivatives have been evaluated in sodium dodecyl sulfate (SDS) in flocculation process. However, N-acylated chitosan was not used as an emulsifying agent while its ability to adsorp on fatty acids was investigated (Lee, et al. 2005). Therefore in this study, hydrophobic partially N-acylated chitosan (PNAC) was produced as a modification to provide hydrophobic attraction with oil surface and chitosan and influence the O/W interfacial properties to affect the sub-processes of emulsification process.

1.4. Scope of the Study

The aim of this study was to produce biopolymeric emulsifiers (partially N-acylated chitosan) and use in oil/water emulsion systems. For this purpose, chitosan was used as a raw material due to its high biocompatibility. The produced emulsifiers were characterized by the following methods: Elemental Analysis, IR Spectroscopy, degree of substitution analysis, X-Ray Diffraction (XRD), Scanning Electron Microscopy (SEM), Surface tension, O/W interfacial tension and contact angle measurements.

To study the effect of these biopolymeric emulsifiers on the kinetics of oil dispersion in water, a set-up was designed to carry out *in-situ* size distribution measurements as a function of time by using light scattering. This set-up was consisted of a standard vessel with four baffles and turbine type stirrer. The following parameters;

- oil concentration,
- chitosan concentration,
- modified chitosan concentration,
- type of chitosan modification (the type of substituted groups),
- acid concentration used to dissolve chitosan and modified chitosan,

were investigated to determine the effects on the kinetics of dispersion of oil in water.

In addition, a phenomenological dispersion model was used to analyze and discuss the kinetic size distribution data obtained in this study.

CHAPTER 2

EMULSION AND EMULSIFICATION PROCESS

2.1. Expression for Emulsion

In literature there exist many definitions about emulsions and types of emulsions but most accredited defition was expounded by UIPAC in 1972 and express that "An emulsion is a dispersion of droplets one liquid in another one with which it is incompletely miscible. Emulsions of droplets of an organic liquid (oil) in an aqueous solution are indicated by symbol O/W and emulsions of aqueous droplets in an organic liquid as W/O. In emulsions the droplets often exceed the usual limits for colloids in size.

Emulsions can be classified as mono-dispersed emulsions and multiple emulsions. Those classifications depend on the nature of continuous and dispersed phase. In the mono-dispersed emulsions there exist oil-in-water (o/w) and water-in-oil (w/o) types. In the case of o/w emulsion the oil is dispersed in the continuous phase water whereas in the w/o emulsion the case is reverse.

2.2. Stability of Emulsion

Emulsion stability is the ability of an emulsion to resist changes in properties of emulsion over time (MCClement 1999). It means that the more stable the emulsion, the more slowly its properties changes. The stability of emulsion is directly related with the droplet-droplet interactions. The droplet-droplet interactions contain; Van der Waals interactions, electrostatic Interactions, hydrophobic interactions, short range forces (Akoh and Min 2008).

Most properties of emulsions are determined by the interaction of the droplets with each other. If droplets attract each other strongly, they tend to aggregate, but if the droplets strongly repelled they tend to remain as apart from each other. Knowledge of the origin and nature of interactions are important in order to provide stability and

physicochemical properties. Droplet-droplet interactions are characterized by an interaction potential ΔG(s) that describes the overall interaction potential obtained by the sum of all various attractive and repulsive effects ((2.1).

$$\Delta G(s) = \Delta G_{VDW}(s) + \Delta G_{electrosatatic}(s) + \Delta G_{hydrophobic}(s) + \Delta G_{shortrange}(s) \quad (2.1)$$

ΔG_{vdw}, $\Delta G_{electrostatic}$, $\Delta G_{hydrophobic}$, and $\Delta G_{short\ range}$ refer to energies related with Van der Waals, electrostatic, hydrophobic, and short-range forces.

Van der Waals Interactions are given always attractive and act between all emulsion droplets types. At close distances the Van der Waals equation given in Equation (2.2) described as;

$$\Delta G_{VDW}(s) = -\frac{Ar}{12s} \quad (2.2)$$

In the equation r is the equal radius of two emulsion droplet, s is the distance between two droplets and A is the Hamaker parameter that depends on the physical properties of the oil and water phases. The strength of interaction increases as the size of the emulsion droplets increases. Van der Waals equation gives an overstated result because it ignores the electrostatic effects, the presence of droplet membrane on the Hamaker parameter.

Electrostatic Interactions are caused by the electrically charged surfaces of the droplets. The electrostatic interaction between two close droplets is given by the Equation (2.3);

$$\Delta G_{electrostatic}(s) = 4.3x10^{-9} r\Psi_0^2 In(1+e^{-4.5}) \quad (2.3)$$

where ψ_0 is the surface potential, r is the radius of droplet. The strength of interaction between two droplets increases as the magnitude of surface potential increases and the size of the emulsion droplets increases. In most of emulsion the droplets have electrical charge and as a result of this they repel each other. Therefore electrostatic interactions are important for preventing droplets from aggregation.

Hydrophobic Interactions are caused by the attractive interactions between nonpolar groups or uncovered surfaces of droplet membrane and water .The interaction

potential energy (Equation(2.4)) between two hydrophobic surfaces separated by water is given by;

$$\Delta G_{hydrophobic}(s) = -0.69x10^{-10} r\Phi \exp(-\frac{s}{\lambda_0}) \quad (2.4)$$

where Φ is the droplet surface fraction (which is hydrophobic) and the decay length, λ_0 is of the order of 1-2 nm. The hydrophobic interactions between droplets play important role in determining the stability of emulsion because attraction between droplets with nonpolar surfaces is strong and relatively long range.

Short-Range Forces result from interactions of two sufficiently close droplets' interfaces starts to interact. These interactions include steric, hydration, protrusion and undulation forces which are sensitive to the size, shape, conformation, packing, interactions, mobility, and hydration of molecules in the adsorbed layer. These interactions are usually repulsive and have ability to increase when the interfacial layers overlap.

These main interactions cause physical and chemical instabilities.

Physical instability results from the organization changes of structures of molecules such as; creaming, flocculation, coalescence.

Chemical instability is caused by the alteration in the chemical structure of the molecules such as; oxidation and hydrolysis are common processes results of chemical instability.

In this study physicochemical instabilities are concerned so in this part the basis of the instabilities such as major effects, methods for controlling them will be briefly summarized.

2.2.1. Creaming

The difference in density of continuous and dispersed phase causes creaming in emulsion. The rate of creaming (υ) (Equation (2.5) depends on the droplet size (*d*), density difference ($\Delta\rho$) between dispersed phase and continuous phase, and the viscosity (η) of the medium and expressed by Stokes' equation (Kinsella 1990):

$$v = \frac{\Delta \rho g d^2}{18\eta} \tag{2.5}$$

The creaming can be slowed by minimizing density difference between the dispersed and continuous liquids. This could be supplied by matching the densities of the oil and aqueous phases. Minimizing droplet sizes in oil-in-water emulsions are also prevent this gravitational separation. Homogenization and use of emulsifiers can be utilized to provide small droplets. By using emulsifier a relatively thick interfacial layer forms and also this decreases the density difference between the dispersed and continuous phase.

2.2.2. Flocculation

Flocculation is the process which two or more particles aggregate without losing their individuality. In the process the aggregation of particles caused from attractive forces between the particles (Pons 2000).

Emulsion droplets flocculate if the particle energy function is minimized. Emulsifier free emulsions tend to flocculation occurrence because the droplets are not covered by emulsifiers and there is no repulsive force between them that resist Van der Waals attractive force.

The presence of charges on the surface of droplets produces repulsive force that opposes Van der Waals attraction. Depending on the strength of either force the droplets either flocculate or energy barrier is formed that prevents minimization of the droplets interparticle energy function. Therefore surface active agents can be used to affect the interparticle interactions.

2.2.3. Coalescence

In coalescence process two or more liquid droplets come together to form a single droplet by film thinning and film deformation of droplets. The mechanism caused by the moving of emulsions toward its most thermodynamically stable state and the moving involves a decrease in the contact area between the oil and water phases.

Coalescence formation strongly depends on the structure and dynamics of interfacial between continuous and dispersed liquids.

The most appropriate methods of controlling coalescence are related with emulsifier types that are used to stabilize the emulsion, pH, ionic strength or temperature variation of the system. These methods prevent close contact of droplets and deformation of droplet membrane.

When the type of emulsifiers are considered, from the literature large and small molecule surfactants could be handled such as for large molecule surfactants; polymer emulsifiers have been found extremely effective at providing protection against coalescence. The reason have been investigated as the proteins' ability to form small droplet sizes and providing strong repulsive forces due to electrosteric effect, big interfacial tension and formation of highly viscoelastic droplet membranes (MCClement 1999). When small molecule emulsifiers have been investigated as having ability to keep droplets apart rather than preventing the membrane deformation. Such as; nonionic surfactants (Tween) was observed as providing a large steric effect and hydration repulsion (MCClement 1999).

2.3. Methods to Provide Stability of Emulsions

The mechanical energy that is applied during emulsification process is known as homogenization. The homogenization is a physical process which is used to intermingle the oil and water phases and form oil droplets if the emulsion is considered as O/W emulsion. During the homogenization the oil droplets tend to form large droplets by coalescing with neighboring droplets. To prevent the coalescence and provide kinetic stability sufficient concentration of emulsifier should be present while the homogenization is applied.

2.3.1. Homogenization

Homogenization processes have been altered according to the volume of starting material, the desired droplet size distribution, and the required physicochemical properties of the final product. Through the following paragraphs some important

homogenization routes that are widely used are briefly summarized (MCClement 2005 , Leal-Calderon 2007).

2.3.1.1. High Speed Mixing

High speed mixing technique involves the agitation of the oil, water and other ingredients that are placed in a suitable vessel (a few cm^3 for laboratory use and m^3 for industrial use) at high speed. The rapid rotation of mixing disrupts the oil-water interface, provides the liquid becomes intermingled and breaks the oil droplets into smaller ones. Through high speed mixing process efficient homogenization is achieved by horizontal and vertical flows which are mostly provided by using fixed baffles at the inner surface of vessel. The design of high speed mixers' head also determines the efficiency of homogenization process. A variety of mixer head exists, such as, blades, propellers, turbines types. All those types are necessary to provide more uniform mixing with more intense disruptive forces and smaller droplets. In high speed mixing technique droplet size is inversely proportional with increasing homogenization time and rotation speed. The technique is commonly applied in food industry for dispersing oil in aqueous phase with an advantage of less air bubbles occurrence.

2.3.1.2. High Pressure Homogenization

High pressure homogenization method is common for producing fine emulsions especially in industrial applications. High pressure homogenizers are more effective at reducing the size of droplets than creating an emulsion directly from two separate liquids. The coarse emulsion is usually created by high speed mixing then feed into the high speed pressure homogenizer. This type of homogenizers works by forcing emulsions through a very narrow channel under pressure. Breakages of droplets in a high-pressure homogenizer depend on the characteristics of the material being homogenized, the size of the homogenizer and also homogenization nozzle design. Obtained results in the literature indicate that there exist a linear relationship between the logarithm of the homogenization pressure and the logarithm of the droplet diameter (MCClement 2005).

Most high-pressure homogenizers are used to homogenate the emulsions in the food and pharmaceutical industries.

2.3.1.3. Ultrasonic Homogenization

Ultrasonic deformation is another way that is used for homogenization of emulsions. Ultrasonic homogenizers working principle is based on cavitation phenomenon. The cavitation phenomenon is described as coalescence and collapsing of micro-bubbles that are formed by the streaming of the ultrasonic waves in the liquid. The implosion of the vapor phase bubbles generates a shock wave with a sufficient energy to break droplets.

2.3.2. Emulsifiers

Emulsifiers are surface active materials that improve emulsification process in the following ways; (see also Figure 2.1) (Polat, et al. 1999).

Decreasing the oil/water interfacial tension: Adsorption of emulsifiers at the oil/water interface causes a decreasing in interfacial tension that facilitates the production of small droplets during homogenization.

Creating a double layer at the oil/water interface: An electrical double layer can be developed at oil/water interfaces which are caused by formation of surface charged droplets. Emulsifier adsorbed droplets alter the interaction of formed small droplets.

Influencing film drainage: Coalescence of two oil droplets is only possible if the film of continuous phase can drain away during the contact period. The presence of emulsifiers in the continuous phase can change the energy required for drainage and so coalescence rate.

Causing steric interaction: Depending on the emulsifier types, adsorption to the droplet surfaces occurs. As a result of emulsifier types the sections extending outward from each droplet prevent successful coalescence formation. This interaction is called as steric stabilization.

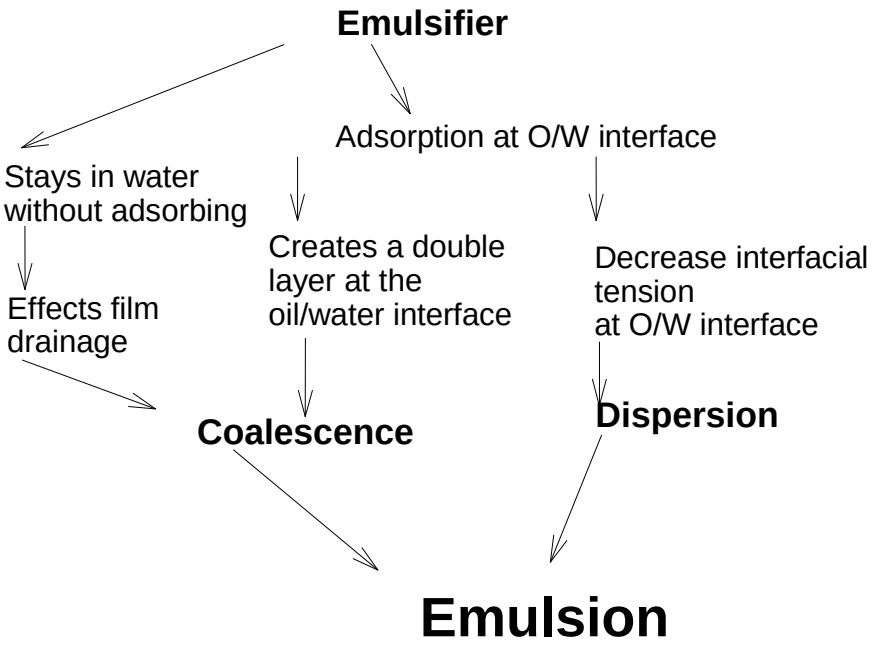

Figure 2.1. Effects of emulsifiers on emulsions.

A wide variety of synthetic and natural emulsifiers are utilized in emulsions. Nowadays a growing trend is observed within the industry to replace synthetic emulsifiers and natural emulsifiers.

2.3.2.1. Synthetic Emulsifiers

Synthetic emulsifiers are usually hydrocarbon derivatives and usually divided into cationic, anionic and non ionic emulsifier groups. Some examples for synthetic emulsifiers are given in following paragraphs (Swarbrick and Boylan 2002).

Cationic emulsifiers; are highly surface-active but less frequently used as emulsifiers. The cation portion based on quaternary ammonium cations including a fatty acid derivative such as oleyaminepolyglycoether which is used for mineral oil, acid cleaners, textile auxiliaries and leather axillaries and stearylaminepolyglcoether which is used for water based adhesives might be given as example for this kind. Cationic emulsifiers are irritating to skin and eyes so not preferred too much.

Anionic emulsifiers; contain anions as the active portion that based on sulfate, sulfanote or carboxylate anions. In general, these emulsifiers are more acid-stable.

Common examples include Sodium lauryl sulfate, triethanolamine sterate which is one of the most popular emulsifiers for creams and lotions in use. Alkykbenzenesulphonate which is universal for cleaning and textile auxiliaries, phosphoric acid esters and its salts which are used for metal degreasing and sulfosuccinates might be given as sample.

Nonionic emulsifiers; this show excellent pH and electrolyte compatibility in emulsions because of the fact that they do not ionize in solutions. Emulsions containing nonionic emulsifiers are generally low in irriation potential, stable and have excellent compability characteristics. Lauryl-myristylalcoholpolyglycoether which is oil soluable emulsifier and used for oil in water emulsion, isodecylalcholpolyglycoether is also oil soluble emulsifier might be considered as nonionic emulsifiers.

2.3.2.2. Natural Emulsifiers

Natural emulsifiers are the ones that are provided us by Mother Nature. Synthetic emulsifiers are widely used in many industrial products but there is an increase in replacing usage of synthetic emulsifiers with natural emulsifiers. Natural emulsifiers might be categorized as low molecular weight and high molecular weight emulsifiers. Monomeric emulsifiers such as mono-diglyceride, lecithin, and glycolipids are considered as low molecular weight natural emulsifiers whereas proteins, polysaccharides (hydrocolloids) and biopolymers are considered as high molecular weight natural emulsifiers (Garti 1999).

2.3.2.2.1. Low Molecular Weight Emulsifiers

2.3.2.2.1.1. Monoglycerides

A glyceride consisting of one fatty acid chain covalently bonded to glycerol molecule through an ester linkage is considered as monoglyceride (Figure 2.2). It is one of the most common emulsifier for water in oil emulsions. Monoglycerides can be used in many food products, cosmetics and pharmaceuticals without any limitations as a result of their hydrophobic characteristic and easy solubility in oils.

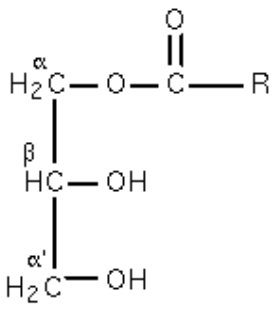

Figure 2.2. Monoglyceride structure.
(Source: Wikipedia 2009)

2.3.2.2.1.2. Lecithins and Lysolecithins.

Phospholipids are amphiphilic molecules because of its hydrophilic head (attracts water) and hydrophobic tail (repels water). As shown in Figure 2.3 the hydrophobic tail consist of long fatty acid hydrocarbon chain.

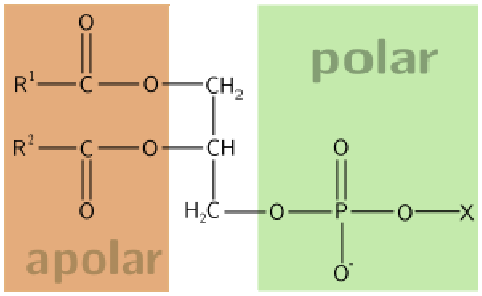

Figure 2.3**.** Phospholipids.
(Source : Wikipedia 2009)

A group of yellowish-brownish fatty substances occurring in animal and plant issues and in egg yolk is called as lecithin which is composed of phospholipids and sphingolipids (certain phospholipids). The phospholipids exist in lecithin (Figure 2.4) tried to be extracted from the materials that contain lecithin such as; soya, wheat, eggs.

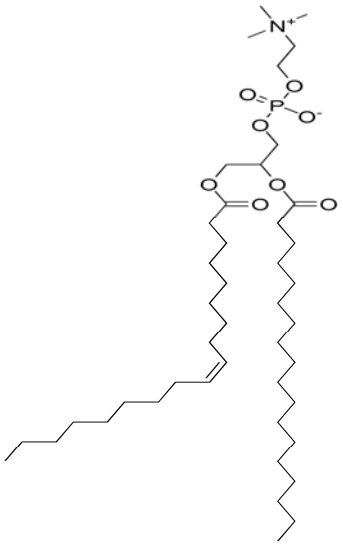

Figure 2.4. An example of of phospholipid in lecithin called as phosphatidylcholine. (Source: Wikipedia 2009)

Lecithin is hydrophobic molecule and hard to use them as emulsifier in water-in-oil or oil-in-water because of the fact it forms lamellar liquid crystallic structures. So the main usage of lecithin are in high concentrations like as; margarine, bread, ice cream, chocolate and etc.

Lysolecithin is a derivative of lecithin that is obtained by hydrophilizing of lecithin. Hydrophilizing of lecithin is performed by attaching hydrophilic functional groups to lecithins' tails such as fatty acid. By this way more hydrophilic structure is obtained that can be used as emulsifier in oil-in water emulsions

2.3.2.2.1.3. Glycolipids

Glycolipids are carbohydrate attached lipids which is shown in Figure 2.5. They occur when phospholipids are combined with non- phosphorous amphiphilic molecules. Those molecules are usually diglyceride ethers with a mono or disaccharides.

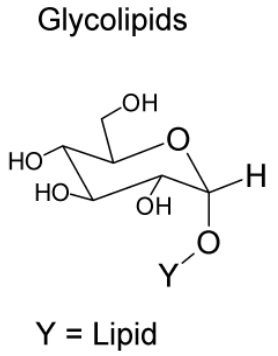

Figure 2.5. Glycolipids structure.
(Source :Wikipedia 2009)

Digalactosyl-diglycreides and triglactosyl-diglycerides are some example of glycolipids that are obtained from cereals (oats, wheat and soya) and have amphiphilic nature. The obtained products are at low yield because but digalactosyl-diglycreides and triglactosyl-diglycerides are thought to be future water-in-oil and oil-in-water natural emulsifiers if advanced separation and extractions methods are investigated.

2.3.2.2.2. High Molecular Weight Emulsifiers

2.3.2.2.2.1. Proteins

The stabilization of emulsions by proteins can be considered as adsorption, denaturation and coagulation subprocesses. Each of these subprocesses needs activation energy, which one overcome result in interfacial tension decreasing (Freiberg, et al.2004).

The proteins that are used as emulsifier can be classified as native proteins and chemically modified proteins.

Native proteins; are known as many proteins such as casein, whey proteins, human serum albumins, gelatins that can be used as emulsifier.

The use of macromolecules can avert creaming but enhance flocculation. But if the homogenization is provided, the native proteins might prevent flocculation either by

electrostatic or steric stabilization. In protein stabilized emulsions if the surface of droplet is poorly covered, bridging flocculation might occur. In many food emulsions the products are composed of combination of monomeric and macromolecular emulsifiers.

Chemically Modified Proteins; active that act as emulsifier are tried to have been made. Many proteins are too hydrophobic or to hydrophilic therefore it's essential to modify them in chemically for rendering them more surfaces.

The functional properties of natural occurring proteins are tried to be enhanced by derivitization whereas the natural occurring proteins have minor limitations in use. For example acylation and alkylation's of amino groups, esterification and amide formation of carbonyl groups and condensation of guanidino groups are some types of modification that are performed. These chemical modifications result in significantly better products than native proteins.

2.3.2.2.2.2. Polysaccharides

The term polysaccharide is also defined as hydrocolloids that is extracted from plants, seaweeds and microbial sources and made by the chemical or enzymatic treatment of biopolymers such as starch, cellulose and chitin (Dickinson 2003). Polysaccharides are good stabilizing agents because of their hydrophilicity, high molecular weight and geletion behavior that cause the macromolecular barriers formation between the droplets in continuous phase. Some of the common polysaccharides that have widely used are gum arabic, galactomannas, and pectin.

Gum arabic; is the most commonly used hydrocolloid emulsifiers and widely used in the soft drinks industry for emulsifying flavour oils.

Galactomannas; is a rather rigid hydrophilic biopolymer with a polymannose and grafted galactose units. Galactomannas are widely used in the food industry as thickening water holding stabilizing agents.

Pectin; are extracted from plant cell, walls and commonly used as gelling and thickening agent in foods.

2.3.2.2.2.3. Biosurfactants

Biosurfactants are any isolated compounds obtained from microorganisms and have influence on interfaces. Biosurfactants are nontoxic, biodegradable and biocompatible so they found too many application areas however they do not lower surface tension and show other classical surfactant properties (Garti 1999). (See Table 2.1. for biosurfactant samples).

Table 2.1. Biosurfactant Type Producing Microbial Species.
(Source: Garti 1999)

A. Glycolipids	
Trehalose mycolates	Rhodococcus erythropolis
	Arthrobacter paraffineus
Trehalose esters	Mycobacterium phlei
	Arthrobacter spp.
	Mycobacterium fortitum
Rhamnolipids	Pseudomonas spp.
Sophorolipids	Candida spp.
B. Phospholipids and fatty acids	
Phospholipids and fatty acids	Corynebacterium spp.
	Micrococcus spp.
	Acinetobacter spp.
Phospholipid	Aspergillus spp.
C. Lipopeptides and Lipoproteins	
Grarnicidens	Bacillus brevis
Polyrnyxins	Bacillus polymyxa
Petide-lipid	Bacilluslicheniformis
D. Polymeric surfactants	
Heteropolysaccharide	A.calcoaceticus A2
Polysaccharide-protein	A. calcoaceticus strains
Carbohydrate-protein	Candida petrophilium
Carbohydrate–protein–lipid complex	Pseudomonas spp.

2.4. Evaluation of Stability

Emulsion stability is generally evaluated with respect to their tendency to phase separation, rheological characteristics, electrical properties and droplets particle size.

Phase separation may be obtained visually. In general, creaming, flocculation and coalescence have occurred before phase separation is visible.

Rheological property determination is often important factor in determining its stability. The droplet size, distribution, degree of flocculation or phase separation results in viscosity changes. Capillary viscometer, cone-plate type device could be used to determine the viscosity changes of emulsions.

Electrical properties of dispersed droplets are often an important indicator for the stability of the system because electrostatic repulsion contributes to prevention of flocculation and coalescence. Therefore the surface charge and zeta potential of emulsified droplets are determined

Particle size of droplets determination is the best way to evaluate stability of emulsion. The particle size and distribution is important because directly affect the characteristic of an emulsion.

2.5. Commonly Used Methods to Determine Droplet Size and Size Distribution

Droplet size and droplet size distribution are two of properties most often used to characterize an emulsion. Most of other properties such as; stability, viscosity and texture are directly related to droplet size therefore; its control is important when studying emulsion. Droplet size, on the other hand, depends on many different factors which are summarized below (Kinsella 1990, Akoh and Min 2008);

Emulsifier concentration: The size of the droplets usually decreases as the emulsifier concentration increases up to a certain level, above this level droplet size remains constant.

Emulsifier type: At the same concentration different types of emulsifiers produce different sized droplets, depending on their surface load, the speed at which they reach the oil-water interface and the ability of the emulsifier membrane to prevent droplet coalescence.

Homogenization conditions: The size of the emulsion droplets usually decreases as the energy input or homogenization time increases.

Besides mean droplet size, characterization of droplet size distribution is also important. Two emulsions with the same mean droplet size might have different size distributions and have different properties.

Several techniques that is given in Table 2.2 are used to determine droplet size such as; direct microscopic observation, electrical sensing zone, single particle optical sensing, sedimentation, light scattering, electrical pulse counters, hydrodynamic chromatography, field flow fractionation and acoustic spectroscopy. These methods have inherent advantages and limitations which can be altered with measurement principles. The summary of these methods will be given with main principles and samples in the following paragraphs.

Table 2.2. Methods for particle size measurement.

METHODS	EFFECTIVE PARTICLE SIZE RANGE (μM)
Microscopy	
Optical	1-1000
Transmission electronic	0.001-5
Scanning electronic	0.01-100
Electrical pulse counting	0.4-400
Sedimentation	
Gravitational	5-150
Centrifugal	0.01-100
Light Scattering	
Dynamic	0.003-2
Elastic(classic)	0.2-2.0
Hydrodynamic Chromatography	0.02-1.5
Field force fractionation	0.002-2

2.5.1. Direct microscopic observation methods

Direct microscopic observation methods are one of the earliest methods that are utilized to observe shape of particles. In early times particle shapes were observed with techniques that have resolution problems therefore the techniques were based on

assumption of all particles were spherical. These older techniques were optical (light) microscopy and ultra microscopy.

The optical microscopy technique provides possibility to observe particles shapes directly. The observation of particles in dispersed systems is restricted by resolving power of the microscope and human errors. Resolving power quality of the microscope intend to proficiency for discrimination of closely packed particles. There also exist available devices with high resolving power that can be used commercially but manual and direct measurement of particles by an analyst might cause human errors and as sample number increases operator errors become common.

Ultra microscopy is the other older technique based on the Tyndall effect which provides visibility for very small colloidal particles. The Tyndall effect is known as light scattering exhibition of colloidal suspensions and this effect is often is shown as an evidence for the presence of colloid. Tyndall scattering caused by reflection of the incident radiation from the surfaces of the particles, from the interior walls of the particles and diffraction of the radiation passes through the particles. As a result of this reflections and diffractions the Tyndall scattering can be only observed when the scattering wavelength is smaller than the particle dimensions that are causing the scattering (The Tyndal Effect 2009). In the ultra microscope technique particles are not directly visible the amount of light depends on the particle volume but the size of a colloidal particle determination is difficult Therefore number concentration of particles are determined either by applying automatic counting or direct counting.

In recent years particle shapes has been determined without residual uncertainty by following up recently developed sufficient techniques For instance; transmission electron microscope (TEM) and scanning electron microscope (SEM) are two of mostly used techniques. In transmission electron microscope obtained images are two-dimensional representation of the particles. In that device operation depends on the electron wave nature and electric and magnetic fields of suitable geometry. Also this technique gives an idea about surface topography about particles with the help of shadow-casting. Generally main problems occur during sample preparation because the structure of samples might decomposed as a result of evacuation in microscope chamber and highly energetic electron bombardment so sample preparation should be achieved with considerations of electrostatic charging, evaporation, melting of sample and decomposition in the beam. The TEM have limitations about showing particles shapes especially providing information about rough surfaces. These limitations are decreased

with the usage of shadowing technique, replication and stereoscopic methods. Stereoscopic methods provide three dimensional images which are applied in SEM technique. In the SEM an electron beam is focused on and deflected across sample surface which causes emission of secondary electrons that are propelled through a collector and detected by a sensitive detector. The SEM is often used to examine structure of sample in detail and provide information about surface composition and limit of resolution is larger than transmission electron microscope.

Optical microscope has some similarities with the electron microscope. The optical microscope uses lenses to control the lights pathway through the system and is in many ways built up like a TEM only the TEM uses electromagnetic lenses to direct the beam of electrons. The TEM and SEM use electromagnetic lenses to control the electron beam (Simple TEM and SEM 2009). TEM and SEM to optical microscope comparison is given in Figure 2.6.

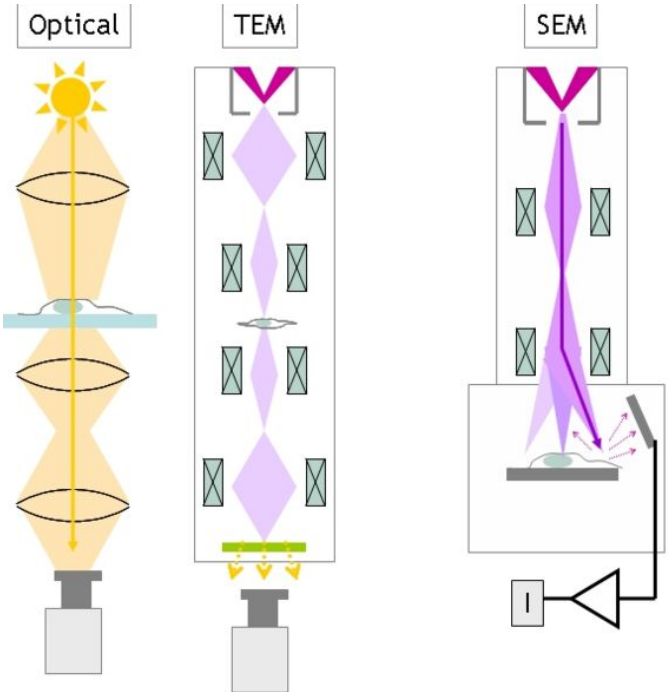

Figure 2.6. TEM and SEM to optical microscope comparison.
(Source: The Simple TEM and SEM 2009)

2.5.2. Sedimentation methods

Sedimentation methods are some of indirect methods for determining particle size of colloidal dispersions that are altered according to sedimentation rate principles. Sedimentation can be considered under two headlines which are; under gravity sedimentation and centrifugal sedimentation. In sedimentation under gravity method dense material sedimentations are easily measured and sufficient especially for particle sizes smaller than 1 μm and dilute colloidal systems smaller than %1.The method can be utilized in various forms;

a) By measuring concentration of particles as a function of time. In this form particles concentration remains constant for a time than falls nearly to zero because during sedimentation process particles decline in measuring zone. The concentration in measuring zone might be determined by using light adsorption and pipette.
b) By determining the change in density of colloidal system at a certain height. Hydrometer or Cartesian diver might be used to detect the density. The divers have been generally preferred for detection because hydrometer shape makes it to locate to the certain height whereas there exist a number of different divers types.
c) By measuring collected deposit mass as a function of time. The mass of deposit is measured by allowing the deposit to pile up on a balance pan placed in dispersion system.

One of these forms might be applied to consider gravity sedimentation. This method application is limited because of time requirement especially for small colloidal particles. For this reason necessity of increase in sedimentation rate rises and particles are exposed to centrifugation. However increasing rate of sedimentation, it is hard to analyze exact particle size distribution since varying the velocity of particles with the particle size and distance from the centrifuge rotator axis. After all sedimentation applications some software systems to calculate the particle sizes and particle size distributions exist.

2.5.3. Electrical pulse counting method

Electrical pulse methods are designed to count to particles number in a known volume of electrolyte solutions. Coulter Counter (shown in Figure 2.7) is the best known electrical pulse counting method that measurement is achieved by dragging the particles through a aperture that separates two electrodes and particles are exposed to current flow while passing through the aperture and resistance changes is amplified as voltage pulses and counted. The Coulter Counter principle assumes that only one particle enters the aperture at a given time and the pulse change is directly proportional to the tri-dimensional volume of particle (Beckham Coulter 2009).

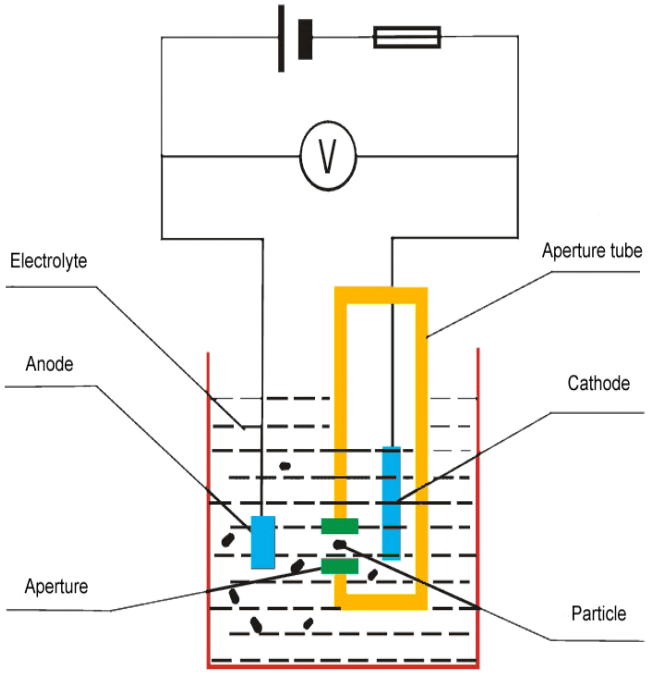

Figure 2.7. Illustration of Coulter Counter instrument
(Source: University of Oslo 2009)

2.5.4. Light scattering methods

When electromagnetic radiation strikes a particle it might absorbed, transmitted, scattered, reflected, or diffracted. From this point of view colloidal systems also scatter

a beam of light and the scattering pattern of light depends on the particle and on the wavelength of light. The older methods were districted to uniform size and simple shape particles whereas light scattering methods can be used for determination of size of particles with different shapes.

There have been two types of techniques that are applied in light scattering particle sizing instruments (Figure 2.8Figure 2.8) scattering (SLS) and dynamic light scattering (DLS). The SLS is defined as technique in which a laser takes place as the light source, acquires particle size information from intensity characteristics of the scattering pattern. The DLS is based on the advantage of the Brownian motion of particles how is; the particles Brownian motion interfere the scattering light intensity fluctuations that are detected and passed to an autocorrelator. The decay characteristics of the autocorrelation function are analyzed to deduce the hydrodynamic radii of sample particles.

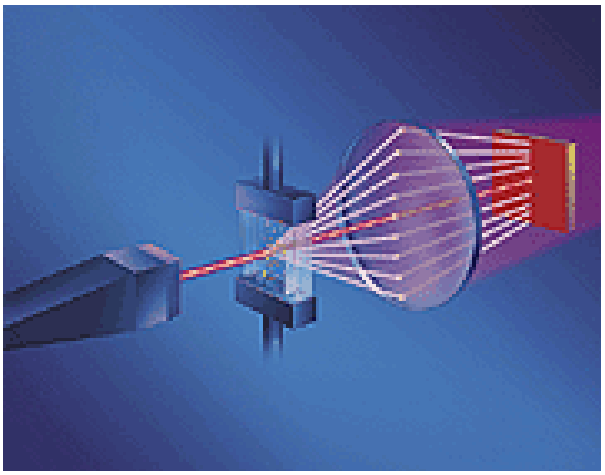

Figure 2.8. Schematic Representation of Light Scattering Process
(Source: Particle &Surface sciences 2009)

The main advantages of light scattering methods are being rapid, nondestructive for particle size measurements and average particle sizes can be estimated without calibration.

2.5.5. Hydrodynamic methods

Hydrodynamic methods are concerned with the separation of particles according their sizes by relating with speeds of particles during elution. The particles in a liquid dispersion are forced to flow under pressure through a packed column with different speeds that is altered by particle sizes which small particles move slowly through the packed column. The particle concentrations in collected fractions are determined as in chromatography. Recently capillary hydrodynamic fractionation (CHDF) and field flow fractionation (FFF) techniques take the place of hydrodynamic chromatography. In the CHDF technique sample is forced to move through capillary tube under pressure that provides opportunity separation for smaller particles whereas hydrodynamic chromatography. It is convenient for determining the particle size of multimodal systems since the individual fractions coming from capillary tube are separated in time and can be detected by visible or UV absorption. Besides this field flow fractionation is also another version of this method which depends on the types of applied field in the channel where the suspension is injected on. These applied fields might be gravitational, electrical, magnetic, and thermal or cross-flow which should be at right angles according to flow.

When advantages of hydrodynamic methods are considered one of the important one is the ability of determining the particle size in dispersion medium which may contain additives such as electrolytes, dispersants or thickeners.

2.6. A Phenomenological Dispersion Model (Polat, et al. 1999)

In emulsion systems knowledge of the maximum stable droplet size (X_{max}) is important in order to control the process. In many studies droplet size distribution was tried to be predicted by using mathematical models under stability or as a function of agitation time. In Hinze's study [1995] it was suggested that a droplet would be disrupted if the ratio of internal and external stress caused by the interfacial tension reaches a critical value. In the literature an empirical dispersion model was developed by using Hinze's approach given in Equation(2.6) (Shinnar 1961).

$$X_{max} = D_i C(We)^{-0.6} \tag{2.6}$$

where D_i is the impeller diameter that is used to agitate the system (this will be discussed in Chapter III, C is a constant and W_e is the Weber number (Equation (2.7)) which is defined as;

$$We = \rho N^2 D_i^3 \gamma^{-1} \tag{2.7}$$

where N is impeller speed in terms of revolution per unit time and ρ is the density of continuous phase. In this proposed model the viscous properties of the dispersed phase was neglected whereas; an alternate model taking the properties of the dispersed phase into account was also proposed to predict the maximum stable droplet size in the presence of surfactants (Ligisetty, et al.1986 , Koshy, et al. 1988).

Other approaches have also been used to estimate the droplet size distribution in an agitated vessel. One of the approaches is the determination of the probability of breakage rate based on similarity concept which had been utilized by the experimental measurements of drop distributions along with a population balance (Narshimhan, et al.1980).

The emulsification model developed by Polat, et al. 1999 correlates the median droplet size of oil with the time of dispersion. The model includes two empirical parameters, the median droplet size at 1 minute of dispersion and a dimensionless breakage rate. Expressing the emulsification data using two distinct parameters is of significant value in the evaluation of process kinetics. The model was developed following Hinze [1955] who suggested that breakage of an isolated droplet is determined mainly by the ratio of external and internal stresses acting on such a droplet. The external stress τ is the force per unit surface area and acts such a way to cause deformation on the droplet. However, the interfacial tension γ will give rise to a surface force that will counteract the deformation. If X is the diameter of the droplet, the internal stress due to the surface tension force will be of the order of magnitude [γ /X]. Hinze proposed that the probability of breakage would be related to a generalized Weber number (Equation (2.8)) which is defined as the ratio of external and internal stresses such that:

$$\mathrm{We} = \frac{\tau \, \mathrm{X}}{\gamma} \tag{2.8}$$

Hinze stated that: " The greater the value of We, that is, the greater the external force τ compared with the counter acting interfacial tension-force γX^{-1}, the greater the deformation. At a critical value $(We)_{crit}$, breakup occurs."

As discussed above, this approach was used by other investigators (Shinnar 1961; Sprow 1967, Lagisetty, et al. 1986; Koshy, et al. 1988) to develop an empirical dispersion model to predict the maximum stable droplet diameter, X_{max}, under steady state conditions.

In a standard vessel with 4 baffles and the agitation speed at 1000 rpm the flow regime is turbulent (1000 rpm). In such a system there will be a distribution of eddies (Walstra 1983) of various sizes which induce the external stresses that lead to deformation of droplets. The efficiency of breakage is a function of both the size of eddies and the droplets. Glasgow, et al. 1985 states that:

> ….clearly, large eddies cannot break small drops and small eddies cannot break large drops. Further, little energy is contained at very small scales that little or no breakage can occur for comparable entity sizes. Thus, a practical limit for particle size reduction in a given system is a length scale on the order of the Kolmogorov(s) microscale (of turbulence)…

If the energy input into the dispersion vessel is constant, it is reasonable to assume that the distribution of eddy sizes will be relatively stable, resulting in a time-invariant microscale of turbulence. Nevertheless, the average droplet size will gradually decrease with time. If the microscale of turbulence is comparable to the droplet size, a significant and increasing fraction of droplets with sizes less than the microscale of turbulence will be generated during the dispersion process. In other words, the number of effective eddies, hence the breakage rate, should be expected to decrease as a function of time. Hence, it could be suggested that the rate of change in the droplet size would be inversely proportional to the dispersion time. The functional form, which is not known, could be estimated from actual emulsification experiments. After calculating the Kolmogorov's microscale of turbulence, λ_0, for the system, one could experimentally determine the fraction of droplets which are finer than λ_0, $F(\lambda_0, t)$, as a function of time. The functional relationship between breakage rate and the dispersion time could be estimated from a plot of $F(\lambda_0, t)$ versus t. This exercise has been carried out for a system as follows:

By dimensional analysis given in Equation (2.9) Kolmogorov (1949) suggested that the dissipation rate, ε, (as shown in Equation (2.10)) and kinematic viscosity, ν, can be arranged to give a length-scale for the turbulence, λ_0, in the system.

$$\lambda_0 = \left(\frac{\nu^3}{\varepsilon} \right)^{\frac{1}{4}} \tag{2.9}$$

$$\varepsilon = \frac{P}{m} \tag{2.10}$$

where ν is the kinematic viscosity, P is the power input into the system and m is the mass of the medium in the tank. Power input (Equation (2.11)) is given by:

$$P = N_p D_a^5 N^3 \rho \tag{2.11}$$

where N_p is the power number which is a function of the Reynolds number[1]. The change in the fraction of droplets which are finer than $\lambda_{0\,(\mu m)}$ as a function of time give that the fraction of droplets that fall below the microscale of turbulence increases linearly with time, with the exception of very short times at which this quantity increases rapidly. This means that the breakage rate will be inversely proportional to the first power of time.

Using the two hypotheses presented above, Hinze's criterion and the inverse relationship between the breakage rate and the time of dispersion, a phenomenological model is proposed. If breakage is dominant, the change in the mean droplet size with time will be proportional to the generalized *We* defined by Hinze while it will be inversely proportional to dispersion time. That is given in Equation (2.12) ;

$$\frac{d}{dt}\left[X_{50}(t)\right] = -k' \left[\frac{\tau(t) X_{50}(t)}{\gamma} \right] \frac{1}{t} \tag{2.12}$$

where $X_{50}\,(t)$ and $\tau(t)$ are the mean droplet size and the external stress per unit area at time t, respectively. γ is the interfacial tension and k' is a proportionality constant. Assuming that $\tau(t)$ can be replaced with a time-averaged stress per unit area, τ

[1]The Reynolds number for an agitated vessel is given as $Re = \rho D_a v_a \mu^{-1}$ where v_a is the tip speed of the impeller ($v_a = 2\pi r N$ where r is the radius of the impeller) and μ is the viscosity of the continuous medium.

(Tatterson, 1991), *k'*, *τ(t)* and γ could be collected as a new, dimensionless constant *k*. It follows Equation (2.13);

$$\frac{d}{dt}\left[X_{50}(t)\right]=-k\frac{X_{50}(t)}{t} \tag{2.13}$$

where $k = k'\frac{\tau(t)}{\gamma}$, integration of Equation (2.13) yields Equation (2.14) ;

$$\ln\left[X_{50}(t)\right]+\ln(C)=-k\ln(t) \tag{2.14}$$

where *C* is the constant of integration. Defining $X_{50(t=1)}$ as the mean droplet size at *1* minute of dispersion, one can determine the constant *C*. Hence,

$$\ln\left[X_{50}(t)\right]=\ln\left[X_{50}(1)\right]-k\ln(t) \tag{2.15}$$

A plot of $ln[X_{50}(t)]$ versus *ln(t)* should result in a straight line with an intercept of $ln[X_{50}(t=1)]$ and a slope of *k*.

2.7. Properties of Alternative Emulsifier Chitosan

Chitin is natural mucopolysaccharide and the supporting material of crustaceans, insects, etc. Chitin is well known to consist of 2-acetamido-2-deoxy-β-D-glucose through a β (1→4) linkage and functions as a structural polysaccharide. It is a white, hard, inelastic, nitrogenous polysaccharide and the major source of surface pollution in coastal areas.

Chitosan is obtained by the *N*-deacetylation of chitin. N-deacetylation is achieved by high concentration of NaOH solution and heat treatment but this *N*-deacetylation is most never complete. The structures of chitin, chitosan and cellulose are shown in Figure 2.9.

Most of the present-day polymers are synthetic materials; their biocompatibility and biodegradability are much more limited than those of natural polymers such as cellulose, chitin, chitosan and their derivatives. However, these natural materials have limitation in their reactivity and process ability (Illum 1998, Amass 1998). In this

respect, chitin and chitosan are recommended as suitable functional materials, because these natural polymers have excellent properties such as biocompatibility, biodegradability, non toxicity, chelating properties, etc.

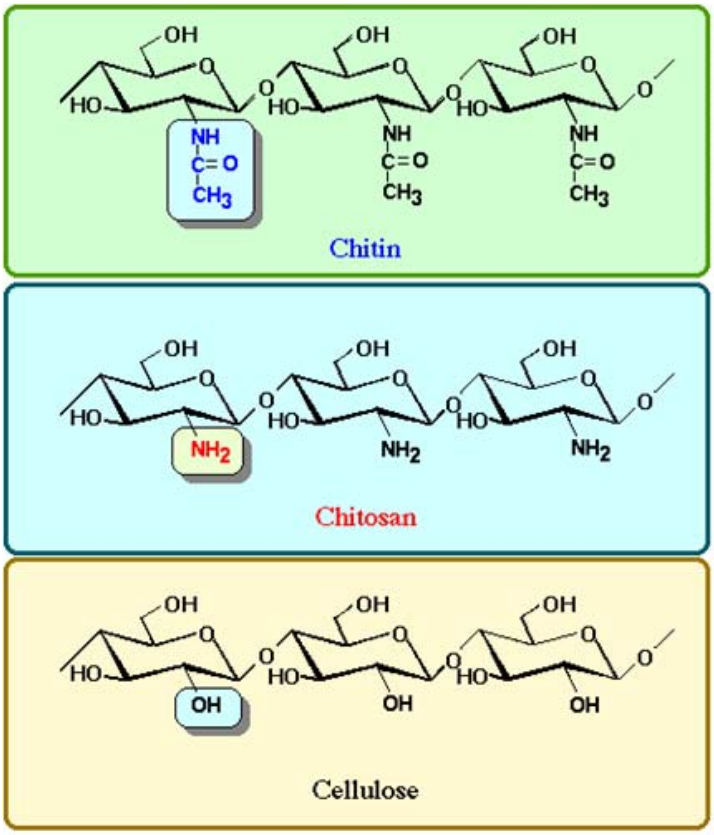

Figure 2.9. Chemical structures of chitin, chitosan and cellulose
(Source: Dallwoo-Chitosan Corparation, 2009)

Most of the naturally occurring polysaccharides, e.g. cellulose, dextran, pectin, alginic acid, agar, agarose and carragenans, are neutral or acidic in nature, whereas chitin and chitosan are examples of highly basic polysaccharides. Their unique properties include polyoxysalt formation, ability to form films, chelate ions and optical structural characteristics (Hench 1998).

Chitin functions naturally structural polysaccharide, but differs from those in its properties. Chitin is highly hydrophobic and is insoluble in water and organic solvents. However, chitosan is soluble in dilute acids such as acetic acid, formic acid, etc. The nitrogen content of chitin varies from 5 to 8% depending on the extent of deacetylation,

whereas the nitrogen in chitosan is mostly in the form of primary aliphatic amino groups. Chitosan, therefore, undergoes reactions typical of amines, of which *N*-acylation and Schiff reaction are the most important (Dutta, et al. 2004).

The great potential for application of chitosan is reflected by the coexistence of several patent applications, in addition to a much higher number of scientific articles which have appeared in the literature during the past decade. Many of the claims suggest replacement of existing synthetic or natural polymers with chitosan (Peter 1995). The most frequently cited advantages of chitosan are seen in the unique physico-chemical and biological properties of the polymer, including antimicrobial activity and biodegradability. The commercial exploration of chitosan has been particularly successful in cosmetics, the manufacture of textile and dietary health food productions.

CHAPTER 3

EXPERIMENTAL

3.1. Materials

In this study, analytical grade chemical were used only. High molecular weight, chitosan powder used to prepare partially N-acylated chitosan was obtained from Sigma Chemical Company. Acetic acid used to prepare 1% (v/v) aqueous acetic acid solution was obtained from Sigma Chemical Company. The other liquids, methanol, ammonia, diethyl ether were supplied by Riedel-de Haen, Merck, Sigma-Aldrich Chemical Companies. Acid anhydrides, valeric and benzoic anhydrides (Figure 3.1) used for the modification of chitosan were supplied by Aldrich Chemical Company.

Dodecane used in emulsification studies was analytical grade and obtained from Sigma Chemical Company. The other reagents like Sodium Hydroxide-NaOH and Hydrochloric acid-HCl were used in the potentiometric titration method to determine the free amine groups in the chitosan were also obtained from Sigma Chemical Company.

All reagents were stored in glassware and polyethylene-polypropylene containers.

Ultra-pure water (18.2 MΩ) was used throughout the study. %10 HNO_3 solution and diluted ethanol solutions were used to clean the used glass wares and deionized water was used to rinse.

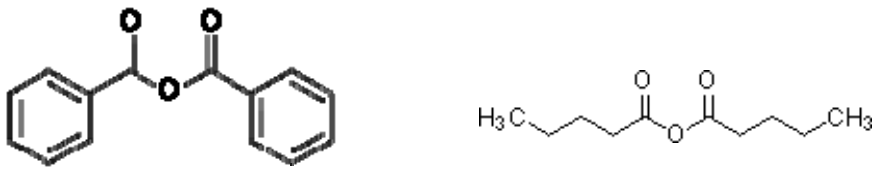

(a) (b)

Figure 3.1. Structure of (a) benzoic anhydride (MW 226.23 $gmol^{-1}$) and (b) valeric anhydride (MW 186.25 $gmol^{-1}$) (Source: Sigma Aldrich 2009)

3.2. Methods

3.2.1. Production and Characterization of Partially N-acylated Chitosan

3.2.1.1. Production

Chitosan derivatives were obtained by partially N-acylation because chitosan has highly reactive free amine group offer great potential for N-acylation (Ramos, et al. 2002). Two type of acid anhydride was used for the N-acylation. These were valeric and benzoic anhydrides. For this reason, chitosan was treated with these reagents. A mixture of chitosan (1g) and 100 ml aqueous acetic acid 1 % (v/v) solution was stirred overnight to ensure total solubility and then diluted with 20 ml. of methanol. Molar equivalent (0.1, 0.5, and 1) of valeric and benzoic anhydrides to one glucoseamine residue was dissolved in methanol as ratio of 2% (w/w) (Lee, et al.1995). After that acid anhydride dissolved methanol solution was poured into chitosan solution and stirred for 1 hour. Then a mixture of methanol aqueous solution of ammonia (7/3, v/v, 100 ml.) was added to chitosan-acid anhydride solution and polymer precipitate was obtained. Then the polymer precipitate was filtered off, washed with methanol and with diethyl ether in order to get rid of unreacted acid anhydrides. Finally obtained precipitates were dried at 40^{o}C under vacuum for two days. The expected change in chitosan glucoseamine residue structure was as following Figure 3.2 (Lee, et al. 2005).

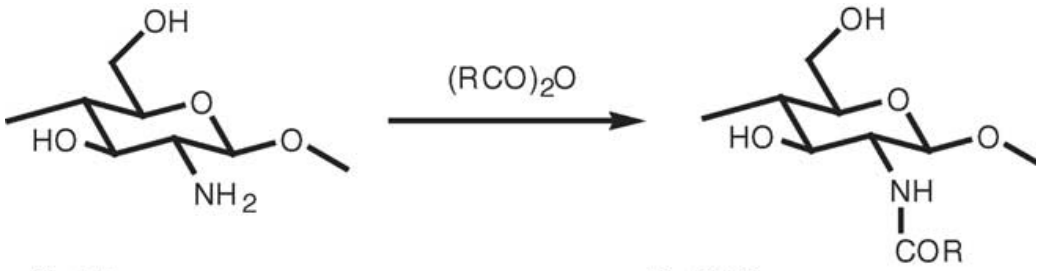

Figure 3.2. N-acylation of chitosan with acid anhydride.

3.2.1.2. Characterization of Partially N-Acylated Chitosan

Physical and chemical properties of commercial chitosan and produced partially N-acylated chitosan (PNAC) were investigated by using various methods.

First of all, molecular weight and degree of deactylation of the commercial chitosan were determined. Then, potentiometric titration and ninhydrin assay methods were applied to obtain substitution degree of alkyl chains and benzene rings to chitosan glucoseamine residues. Elemental analysis method was used for determination of the changes in C/N ratios that also gives information about the degree of substitution. IR spectroscopy was used for qualitative observation of substituted groups during synthesis. Crystalline structure, forms of the materials and images were also obtained with the help of X-ray diffractometer and scanning electron microscope (SEM).

3.2.1.2.1. Molecular Weight Determination of Commercial Chitosan

Viscometry was used to evaluate the molecular weight of chitosan. The method is one of the simplest and most rapid methods. The intrinsic viscosity of polymer is related to its molecular weight according to Mark-Houwink-Sakurada relation (Equation (3.1) (Kasaaı, et al. 2007).

$$[\eta] = KM_{\upsilon}^{\alpha} \tag{3.1}$$

where as $[\eta]$ is the intrinsic viscosity, M_{υ} is the average molecular weight of polymer, K and α are related with percentage of deacetylation degree (DD %) and obtained from the literature. The equations were given below (Equation (3.2) and Equation (3.3));

$$K = 1.64 \times 10^{-30} \times DD^{14.0} \tag{3.2}$$

$$\alpha = -1.02 \times 10^{-2} \times DD + 1.82 \tag{3.3}$$

Hence using these equations, $K=0.104*10^{-3}$ and $\alpha=1.12$ for 69 % DD values were obtained for chitosan used in this study (Wang, et al. 1991).

In addition, the solvent system and the temperature were also depended on DD % of chitosan. Therefore, the corresponding solvent system was acetic acid/sodium

acetate (0.2 M HAc/0.1 M NaAc) at 30^{o}C for DD % 68 (Wang, et al. 1991). Stock solution of chitosan was prepared in a way that 0.25 g chitosan was dissolved in 200 mL of 0.2M HAc / 0.1M NaAc solvent system and lower concentrations (0.0000, 0.0100, 0.0125, 0.0250, 0.0375, 0.0625, 0.0875, 0.1250 w/v) were prepared from this stock solution and diluted with the same solvent. Kinematic viscosity measurements of chitosan solutions were carried out by using PETROTEST kinematic viscosity apparatus; an Ubbelohde U-Tube capillary viscometer with 0.00924 cSt/s^2 viscosimeter constant (C).The capillary viscosimeter was filled with the sample than the sample was passed through the capillary and the running time was measured. Each measurement was repeated for three times. The sample or solvent viscosity was calculated from Equation (3.4) and Equation (3.5).

.

$$\eta_{sample/solvent} = C(mm^2/\sec^2)t(\sec) \tag{3.4}$$

$$\eta_{sample/solvent} = \frac{(\eta_{sample} - \eta_{solvent})}{\eta_{solvent}} \tag{3.5}$$

The reduced viscosity was calculated from Equation (3.6) where c is the chitosan solution concentration used in viscosity measurement.

$$\eta_{reduced} = \frac{\eta_{specific}}{c} \tag{3.6}$$

For the calculation of intrinsic viscosity, Equation (3.7) (Tsaih and Chen 1999) was used that is the intercept of the equation derived from plot of reduced viscosity versus concentration of chitosan solution (g/mL).

$$\eta_{reduced} = [\eta] + k[\eta]^2 c \tag{3.7}$$

The molecular weight of chitosan was calculated according to Equation (3.1) as given before.

3.2.1.2.2. Degree of Substitution Determination

A variety of analytical methods are used to determine the free amine groups in partially N-acylated chitosan such as by Potentiometric titration (Tolaimate 2000), Infrared spectroscopy, Ninhydrin assays (Tien, et al. 2003). In this study, both potentiometric titration and ninhydrin methods were performed to determine the free amine group content. Elemental analysis was also performed to observe C/N changes (Hirano 1980).

3.2.1.2.2.1. Potentiometric Titration

Potentiometric titration method depends on the deprotonation of positively charged free amine groups in chitosan .This method was carried out by dissolving samples in a known excess of hydrochloric acid (HCl) solution and then titration of the dissolved sample with standardized sodium hydroxide (NaOH) solution.

In this part of characterization KYTO Automatic Potentiometric Titrator of KEM AT510 was used. The samples with amount of 100 mg were dissolved in 10.0 mL of 0.2 M HCl and after that being diluted to 30 mL with ultrapure water; they were titrated with 0.06 M NaOH. From the titration a curve with two inflection points are obtained and the difference between them gives the amount of NaOH that is used to deprotonate positively charged amine groups (Tolaimate, et al. 2000). Equation (3.8) was used to calculate amount of NH_2 %.

$$NH_2\% = \frac{16.1(V_2 - V_1) \times M_b}{W} \tag{3.8}$$

where V_1 is the base volume that consumed for the first inflexion point (mL), V_2 is the base volume that consumed for the second inflexion point (mL) and M_b is the base molarity (g/mol) and W is the weight of the sample.

3.2.1.2.2.2. Ninhydrin Assay

The unchanged amino groups remaining after partially N-acylation were determined with ninhydrin assay that was described by Tien, et al.2003. A standard curve was obtained by using initial commercial chitosan with the free amine groups. Synthesized PNAC samples (0.1 mg/mL) were dissolved in acetic acid (3% w/v) and hydrochloric acid (1% w/v) aqueous solution. 0.5 ml. prepared acetate buffer was added to each chitosan solutions. 2 mL. Ninhydrin reagents were added to each solution. The obtained solutions were heated in boiling water bath for 20 minutes. After cooling their absorbances were read at 570 nm by using Varian Cary 50 UV-VIS spectrophotometer.

3.2.1.2.2.3. Elemental Analysis

The most common form of elemental analysis is the determination of C, H, and N contents of samples. The analysis is accomplished by the quantities of CO_2, H_2O and NO_2 produced by the combustion of the dried carbonaceous materials in excess oxygen. The weights of these combustion products are used to calculate combustion of samples. In the elemental analyzer furnace combustion of the samples are performed at 1000^oC. The weight percentage of C, H is determined by infrared detection where as N content is measured by thermal conductivity detection.

In this part of characterization LECO-CNHS-932 elemental analyzer was used to determine C/N ratios of each synthesized materials to observe the substitution changes after N-acylation of chitosan with valeric and benzoic anhydrides.

3.2.1.2.3. Fourier Transform Infrared Spectroscopy (FTIR)

Fourier Transform Infrared Spectroscopy (FTIR) was used for qualitative analysis of PNAC to determine the presence or absence of certain types of bonds and functional groups and also for the calculation of substitution degree. FTIR spectroscopy measures infrared radiation absorption of samples as atoms' bonds vibrate. The absorptions are used to identify bond types, functional groups in compounds.

The degree of substitution was evaluated by FT-IR spectra, Equation (3.9). The ratio of absorbance at 1655 cm^{-1}(ascribed to amide I) band and the hydroxyl band at 3450 cm^{-1}, applying the equation given below; (Tien, et al.2003).

$$DS\% = [(A_{1655} / A_{3450}) - 0.32] \times 100 \quad (3.9)$$

where DS % is degree of substitution and the value of 0.32 represents acetyl groups exist in commercial chitosan.

The structure of PNAC was investigated by using FT-IR spectra that recorded by using Perkin Elmer Spectrum 100 FTIR spectrometer in a frequency range of 4000–400 cm^{-1} with 4 scans at a resolution of 4 cm^{-1}.Samples were prepared in the forms of thin film. For the preparation 2% w/v chitosan and PNACs samples were dissolved in 2% AcOH and poured on Petri dish and dried at 40^{o}C for 24 hours under vacuum.

3.2.1.2.4. X-Ray Diffraction (XRD)

X-Ray diffraction (XRD) is an analytical technique that is used for examining crystalline solids that include ceramics, metals, organics, polymers and etc. By using X-Ray diffractometer the molecular structure of materials and phase identification with quantitative phase analysis might be achieved. The theoretical basis of X-Ray diffraction stands on Bragg's equation given by Equation (3.10(3.10;

$$n\lambda = 2d \sin\theta \quad (3.10)$$

Where n is the order of reflection n=(1, 2, 3,….) λ, the wavelength, *d* the distance between parallel lattice planes and Θ the angle the incident beam and a lattice plane, known as Bragg angle. When the path length in the crystal ($2d\sin\Theta$) is a multiple of the wavelength, constructive interference occurs and diffracted intensity is obtained. The geometry of the crystal lattice determines the position of the peaks in an X-ray diffraction pattern. In general, as the material become more symmetrical, the peaks became fewer in its diffraction pattern. The peak intensities associate with the diffraction intensity that are determined by the arrangement of atoms within the crystal lattice.

XRD analysis was performed by using a Philips X'Pert Pro instrument. X-Ray diffraction data were collected by using Cu anode with 0.154056 nm wavelength (λ) in 5-50 θ. The samples crystallographic properties and the changes in crystallinity of chitosan caused by partially N-acylation was obtained. By using XRD data, the crystal size of samples (t) was also calculated with application of Debye Scherrer equation (Equation (3.11);

$$t = \frac{0.9\lambda}{\beta \cos\theta} \tag{3.11}$$

where *0.9* is the shape factor, λ is the X-Ray wavelength, typically 1.542 Å, β is the line broadening at half the maximum intensity in radians, and θ is the Bragg angle which is the angle of incident beam and lattice plane which comes from the theoretical basis of X-Ray diffraction.

3.2.1.2.5. Scanning Electron Microscope (SEM)

Scanning Electron Microscope (SEM) was used rather than optical microscope to study the surfaces, morphologies and forms of samples because SEM can achieve higher magnifications than optical microscopes.

SEM analyses are conducted in vacuum environments and all non-conductive samples must be coated with electrically conductive coatings before observing with SEM.

In this study, SEM characterization was carried out by using a Philips XL-30S FEG type instrument in vacuum environment. In order to provide conductivity the samples which were placed on metallic disks were coated with Au. The sample surfaces' images were recorded at different areas and magnification.

3.2.1.2.6. Determination of Surface Activity

3.2.1.2.6.1. Surface Tension Measurements

Surface tension is one of the fundamental properties of a liquid, reflecting intermolecular interactions. Surface tension is commonly measured at liquid/gas (mainly air) and liquid/liquid (water) interfaces. Functional properties of surface active materials result from their ability to reduce surface (or interfacial) tension by adsorbing and formation of cohesive films at the interface. The most common method used to determine the surface tension is Du Nouy Ring method in which the interaction of platinum ring with the surface/interface being tested. The ring is submerged below the surface/interface and subsequently raised upwards. As the ring moves upwards it raises a meniscus of liquid and this meniscus tears from the ring. Prior to this event, a maximum force is experienced and recorded in the measurement. At the maximum the force vector is exactly parallel to the direction of motion; at this moment the contact angle θ is 0. The following Figure 3.3 shows the change in force as the distance of the ring increases.

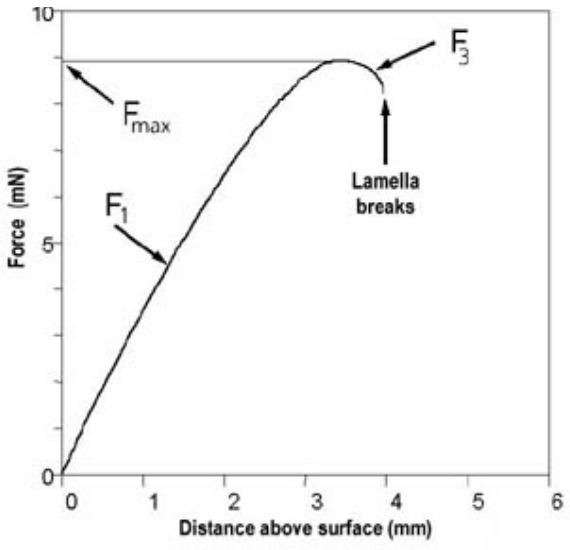

Figure 3.3.The change in force as the distance of the ring increases during surface tension measurement (Source: KRUSS 2009).

The surface tension of the liquid is determined from the measured force using the equation shown in below (Equation (3.12)):

$$\gamma = \frac{(F_w)}{(L \times \cos\theta)} \tag{3.12}$$

where γ is surface/interfacial tension, F_w is the measured force, L is the wetted length of ring and the θ is the contact angle.

In this study, KRÜSS Digital-Tensiometer K10ST was used to measure both the surface (at air/water interface) and interfacial (dodecane/water interface) tensions of several solutions in this study. These solutions were acetic acid solutions (at different concentrations) and PNAC solutions (at different concentration of 0.01% and 0.03% (w/v) in 5% (v/v) acetic acid aqueous solution). These measurements were conducted at room temperature.

3.2.1.2.6.2. Contact Angle Measurements

Contact angle measurement is a simple method for surface analysis related to surface energy and tension. Contact angle describes the shape of a liquid droplet resting on a solid interface. When a tangent line is drawn as shown in Figure 3.4 from the droplet to the touch of the solid surface, the contact angle is he angle between the tangent line and the solid surface.

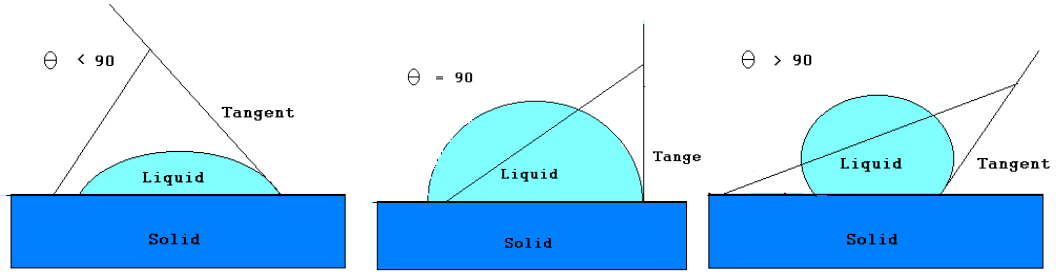

Figure 3.4. llustration of contact angle measurement of solids.
(Source: KSV 2009)

These figures show the wetting properties (the degree of hydrophobicity) of solids. High values of θ indicate poor wetting whereas, low angle values indicate that the liquid spreads and might be said as having ability to wet the solid. A zero contact angle represents complete wetting.

Two different methods are used to measure contact angles of solids. These are; Goniometry that comprises the observation of liquid droplet on a solid surface and tensiometry that contains measuring the forces of interaction as a solid contacted with a liquid.

In this study, KRÜSS Contact Angle Measurement System G10 instrument was used to measure contact angle values in chitosan/air/water and N-acylated chitosan/air/water systems. The basic parts of this instrument are a light source, sample stage and microscope as it is goniometer. Solid disks were prepared from each type of partially N-acylated chitosan (PNAC) for contact angle measurement. Solid disks were prepared before the samples were absolutely dried.

A Gilmont micro-syringe was used to obtain water droplets on the samples' surface. The contact angle measurements were utilized on three different sites of the surface. By this way the data provided information about the distribution of contact angles and for each sample, average of these three measurements was given as a result.

3.2.2. Emulsification Studies

In the present study emulsions were formed in a sampling vessel shown in Figure 3.6 that contain dodecane at 1% (v/v) percentage as dispersed phase and the emulsifying agents at different portions (0.005 ,0.01, 0.02, 0.03 % (w/v)) were dissolved in 5% (v/v) acetic acid aqueous solutions as continuous phase. For homogenization VELP SCIENTIFICA Stirrer type BS agitator was used. The oil droplet sizes were investigated with Malvern Mastersizer 2000 Particle Size Analyzer with the help of J.P. Selecta Peristaltic Pump PR2003.

The size distribution measurements were carried out by in-situ measurements whereas batch measurements are generally applied in literature. In batch measurements a small sample is obtained from the vessel and size distributions are tried to be obtained. This method may not yield the actual size distribution because a finite time passes between the sampling and the measurement. On the other hand, in situ measurements of

the size distribution in a vessel minimize such drawbacks. As a result of this a set-up was designed to carry out *in-situ* size distribution measurements as a function of time using light scattering.

Set-up: A schematic of the experimental set-up for these studies is given in Figure 3.5. It contains a one liter vessel (V) of standard geometry (Holland and Chapman 1966) with four baffles to provide homogeneous mixing and a turbine type stirrer (S). The agitation speed was maintained constant at 1000 rpm .The vessel was connected to a flow-through cell with a 1/8" silicon tubing. There is laser source where the light (I_1) comes from it and the light (I_2) goes to the detector. The flow through cell is present in the light beam path of a light scattering size measurement device (C). An adjustable speed peristaltic pump (P) was used for circulating the solution. Dodecane at a portion of 1% (v/v) was added to the agitated vessel and one minute later size distribution was recorded. The size distributions of droplets were recorded at preset-times these are; 1, 2, 4, 8, 12, 16, 20, 24, 28, 32, 36, 40, 44, 48, 52, 56, 60, 64 minutes.

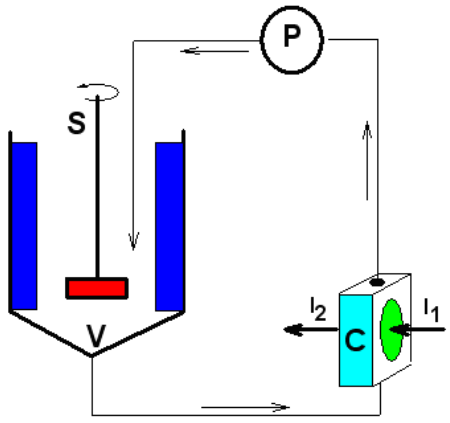

Figure 3.5. Experimental set-up used in the study.

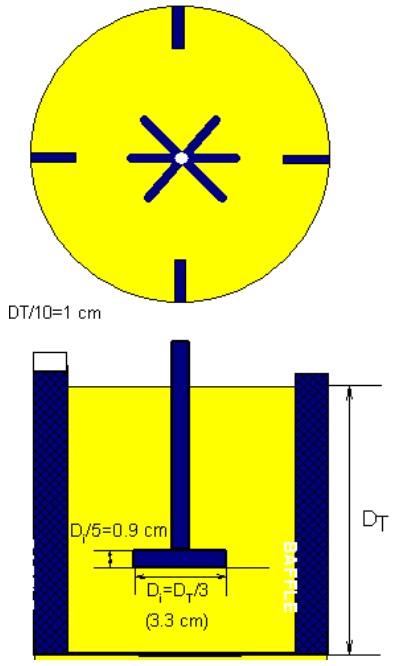

Figure 3.6. Agitation vessel and the turbine type stirrer used in this study

3.2.2.1. Application of a Phenomenological Dispersion Model on Size Data

The droplet size distribution for the emulsification of dodecane droplets in 5% aqueous solution (with modified chitosan as emulsifier 1%) are obtained by the setup described earlier, given in Figure 3.7 as a function of time. The normalized size distributions for the same data presented in Figure 3.8 demonstrates that the size distributions are self-preserving. Therefore to represent the changes in the droplet size, the median droplet size (X_{50}) was utilized. The time dependence of the median droplet size X_{50}, for the data in Figure 3.7 is given in Figure 3.9.

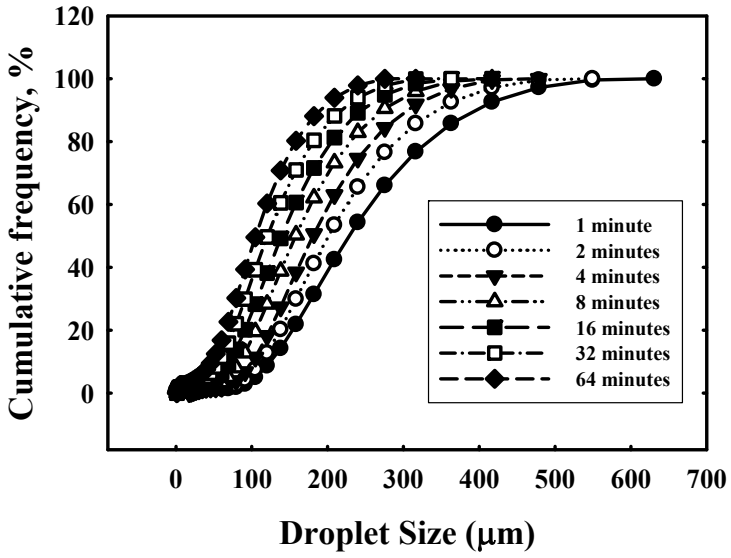

Figure 3.7. Size distribution of oil droplets in 5% aqueous solution (with 0.1 mol ratio valeric anhydride modified chitosan as emulsifier) at various times.

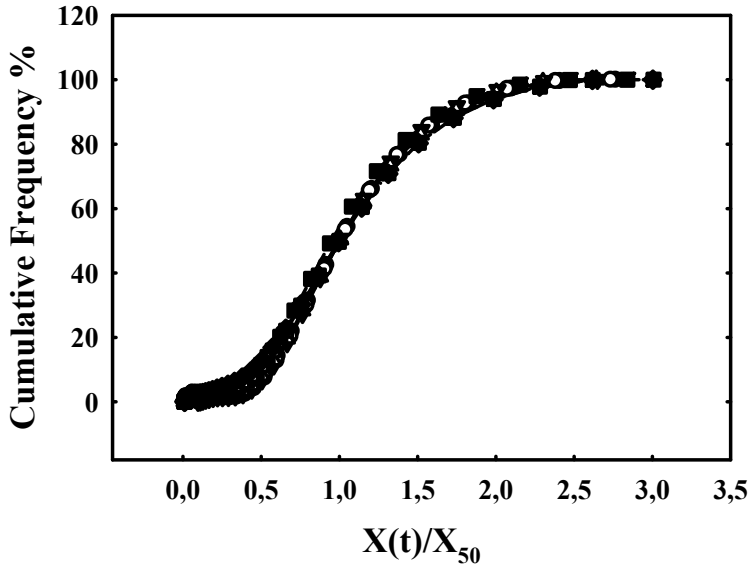

Figure 3.8. Normalized size distribution of dodecane droplets in 5% aqueous solution (with 0.1 mol ratio valeric anhydride modified chitosan as emulsifier) at various times.

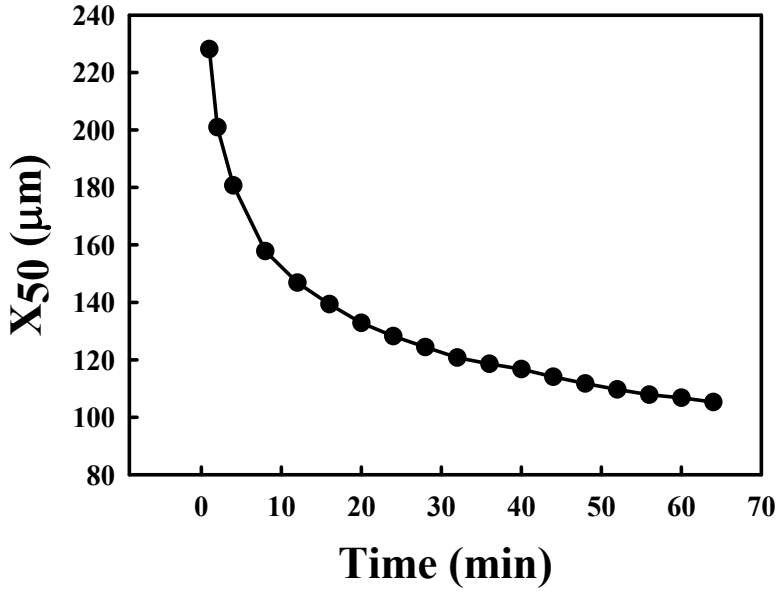

Figure 3.9. Change in the median droplet size, X_{50} as a function of time for 1% dodecane

The median droplet size of oil is related with the time of dispersion as it was utilized in an earlier study (Polat, et al.1999) (as discussed in Chapter 2).

The size distribution measurement set-up discussed above contains a standard vessel with four baffles and the agitation speed at 1000 rpm with turbulent flow regime.

The Kolmogorov microscale (λ_0) of turbulence was calculated in this system in order to determine the fraction of droplets finer than λ_0 as a function of time ($F\ \lambda_{0,}\ t$).

For this, the input power (P) was calculated with the Equation 2.10 suggested by Tatterson (1991).The Reynolds (Re) number for the agitated vessel was calculated by using Equation (3.13).

$$Re := \frac{N \cdot D_i^2 \cdot \rho_W}{\mu} \tag{3.13}$$

where N is the speed of impeller, D_i is the diameter of impeller, N is the speed of impeller tip, ρ_w is the density of continuous phase and μ is the viscosity of the continuous medium. The Reynolds number was calculated as 1.468×10^4 and the power number was given as 4 for this region by Tatterson 1991.

The microscale of turbulence (λ_0) in the system was calculated with the Kolmogorov length-scale suggestion given in Equation (2.8) and Equation (2.9).ε, is the dissipation rate that is calculated with the ratio of power input and mass of the medium in the standard vessel and υ is the kinematic viscosity. These equations give the input power as 0.395 watt and microscale of turbulence about 38 μm.

The fraction of droplets that are smaller than 38 μm as a function of time is given in Figure 3.10. It is seen that the fraction of these droplets is increasing linearly with time so the breakage rate should inversely proportional to the first power of time.

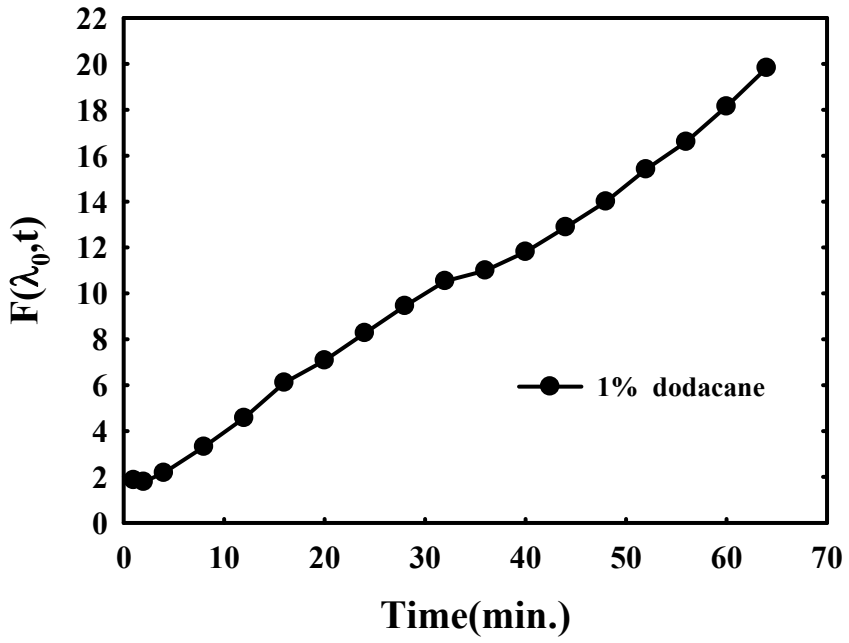

Figure 3.10. A plot of the fraction of droplets those are smaller than λ_0 as a function of agitation time.

CHAPTER 4

RESULTS and DISCUSSION

4.1. Characterization of Commercial Chitosan

4.1.1. Degree of Deacetylation Determination

Elemental analysis and potentiometric titration methods are the most commonly used rapid methods for determination of chitosan deactylation degree.

In elemental analysis the ratios of carbon (C) and nitrogen (N) atoms are tried to be obtained to calculate the degree of deacetylation because in deacetylation process carbon (C) and oxygen (O) atoms removes and nitrogen (N) atom remains constant. For this reason the equation given below is used;

$$DD = 1 - \frac{(C/N - 5.145)}{6.816 - 5.145} \times 100 \tag{4.1}$$

The elemental analysis result for commercial chitosan is summarized in Table 4.1.

Table 4.1. Elemental Analysis Result for Commercial Chitosan

Compound	Sample amount (mg)	C%	H%	N%	S%
Commercial chitosan	2.10	25	40.52	7.20	7.15

The deactylation degree of chitosan was also obtained by the potentiometric titration. A curve with two inflexion points were obtained from the titration of chitosan dissolved hydrochloric acid solution with sodium hydroxide solution. The difference between the volumes of this two inflexion points gives information about the sodium

hydroxide solution that was consumed for the deprotonation of free amine groups. The determination of chitosan deacetylation degree is calculated by using the Equation (4.2) below (Tolaimate 2000);

$$NH_2\% = \frac{16.1(V_2 - V_1) \times M_b}{W} \tag{4.2}$$

where V_1 is the base volume that consumed for the first inflexion point (mL), V_2 is the base volume that consumed for the second inflexion point (mL) and M_b is the base molarity (g/mol) and W is the weight of the sample. The Potentiometric titration graph of chitosan was illustrated in Figure 4.1 where the difference between two inflection points corresponded to amount protonated amine groups in chitosan.

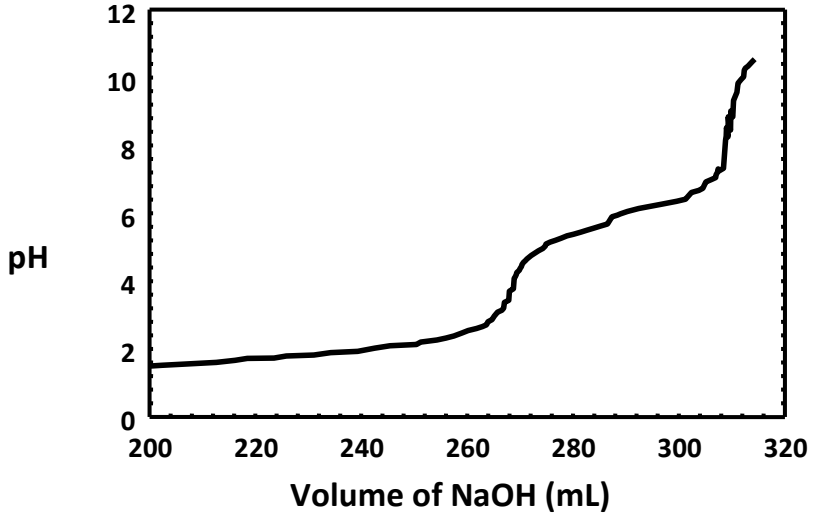

Figure 4.1. Titration Curve of Commercial Chitosan dissolved in (0.2M) HCl with standardized (0.06 M) NaOH solution

From the potentiometric titration that was carried out by automatic titrator device the deacetylation degree was obtained as 61.50 % with the application of Equation (3.8) whereas the elemental analysis result gives the degree of deacetylation as 68.70 %.

4.1.2. Molecular Weight Determination of Commercial Chitosan

Molecular weight of commercial chitosan was determined with the kinematic viscosity measurement and with the application of the Mark Houwink equation;

$$[\eta] = KM_{\upsilon}^{\alpha} \tag{4.3}$$

K and α values were taken as 0.104×10^{-5} (dL/g) and 1.12 respectively which were calculated by Wang, et al. 1991.

Figure 4.2 shows the intrinsic viscosity of commercial chitosan sample used in this study was 10.228 mL/g at acetic acid/ sodium acetate (0.2 M CH_3COOH/ 0.1 M CH_3COONa) solvent system whose molecular weight was calculated as 28.695×10^3 (g/mol).

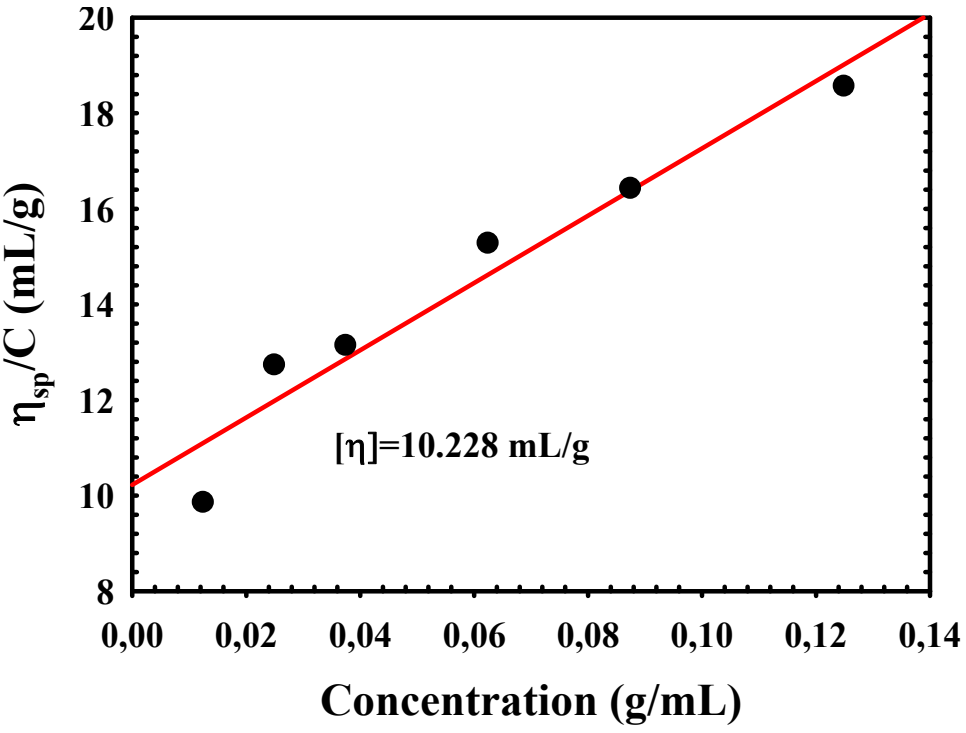

Figure 4.2. Determination of the Intrinsic Viscosity of Commercial Chitosan

Molecular weight result of commercial chitosan was determined as high molecular weight this is the desired property to synthesize partially N-acylated chitosan (PNAC).

The degree of deacetylation and molecular weight of commercial chitosan determinations were calculated as an initial because the obtained results were used in synthesis PNAC.

4.2. Characterization of Partially N-acylated Chitosan

4.2.1. Determination of Substitution Degree

Different methods have been utilized for the determination of substitution degree of partially N-acylated chitosan (PNAC). These methods are ninhydrin assay and elemental analysis and also FT-IR.

Degree of substitution value of PNAC is directly related with the analytical methods employed as in chitosan degree of deacetylation determination.

The unchanged amino groups remaining after acylation were determined by the method Ninhydrin assay (Tien, et al. 2003). The degree of N-acylation was also evaluated by FTIR by applying the equation given below;

$$DS\% = [(A_{1655} / A_{3450}) - 0.32] \times 100 \quad (4.4)$$

where DS % is degree of substitution and the value of 0.32 represents acetyl groups exist in commercial chitosan.

The elemental analysis was utilized to investigate the changes in carbon to nitrogen ratios. The elemental analysis results show an increase in Carbon to Nitrogen ration as the initial mol ratio of modification increases Table 4.2.

Table 4.2. Estimation of degree of substitution by Ninhydrin, FTIR and C/N.

	Degree of Substitution (%)		
Sample	**Ninhydrin assay (%)**	**FT-IR(%)**	**C/N**
PNAC 0.1V	23.74	25.82	5.77
PNAC 0.5V	35.41	37.26	6.03
PNAC 1.0V	45.37	47.66	7.03
PNAC 0.1B	34.23	35.57	5.53
PNAC 0.5B	43.18	44.08	6.18
PNAC 1.0B	44.02	45.37	7.06

4.2.2. FTIR Analysis

The structure of commercial chitosan and PNACs were identified by using FTIR spectra. The spectra of each modification were given in Figure 4.3 and Figure 4.4.

The studies in literature about FTIR spectroscopy related with chitosan and N-acylated chitosan show some characteristic peaks for chitosan. These are; at 2940 cm^{-1} ($-CH_3$,$-CH_2$), 1655 cm^{-1} (C=O stretch vibration of secondary amide I band), 1555 cm^{-1} (N-H bending vibration of amide II band), 1570 cm^{-1} (N-H bending vibration of primary amides), and 1070 cm^{-1} (C-O stretching) (Lee, et al. 2005 and Choi, et al.2007).

After the observations discussed above the spectra between wave number 1700 cm-1 and 400 cm-1 will be closely investigated in

Figure 4.3.b in order to evaluate the exact changes after N-acylation of chitosan for 0.1 inital mol ratio valeric anhydride modification (0.1V PNAC).0.5 mol ratio valeric anhydride modification (0.5V PNAC), 1 mol ratio valeric anhydride modification (1 V PNAC). The peaks observed around 1650 cm^{-1}, 1570cm^{-1} were attributed to secondary amide I and II bands of –CONH- , and as the initial mol ratio of valeric anhydride increases the peak around these values became sharper. These change indicate the increase of stretching vibration of C=O bond in amide I band and also bending vibration of N-H bending vibrations. Other changes were observed in IR bands in the region of 1380 -1460 $cm^{-}1$ which attributes the symmetric and asymmetric bending vibrations of methyl the peaks that are around the wave number in the study of Li, et al. in 1998. The band around 1380 cm^{-1} which is given as strong finger print region of $–COCH_2$- in literature (Williams and Fleming 1987). An observed increment

in the region 1380 cm^{-1} is means that the symmetric vibrations increase whereas the peak around 1460 cm^{-1} remains the same as the initial mol ratio of valeric anhydride increase. When the spectra given in

Figure 4.3.a is observed, the peaks' sharpness in the region of 2933 and 2870 increase as the initial mol ratio of valeric anhydride was increased that is ascribed as increases of $–CH_2$-, $-CH_3$ groups.

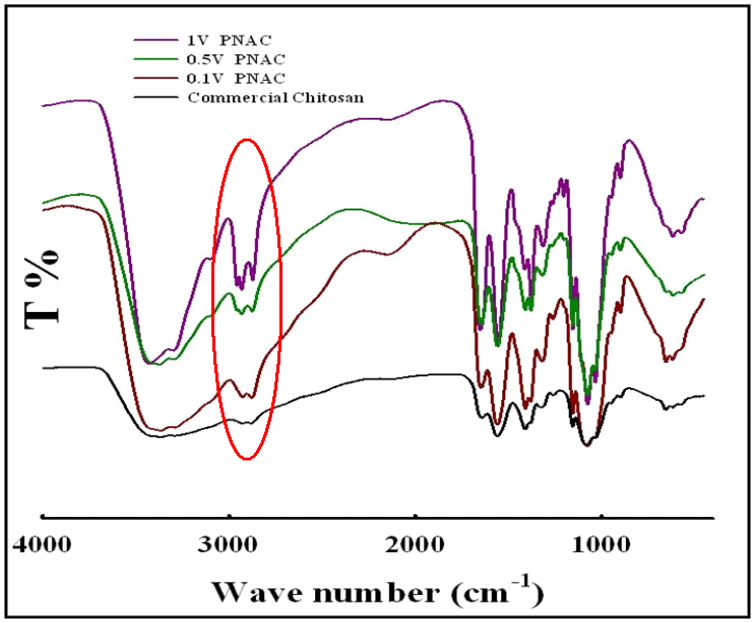

(a)

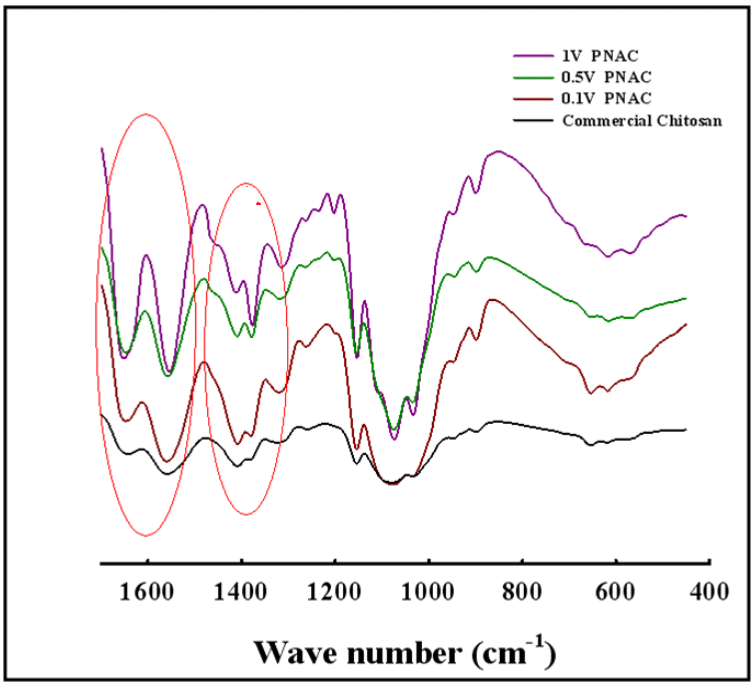

(b)

Figure 4.3. FTIR spectra of commercial chitosan and modified PNACs with valeric anhydride (a) between the 4000–400 cm^{-1} , (b) 1700–400 cm^{-1}.

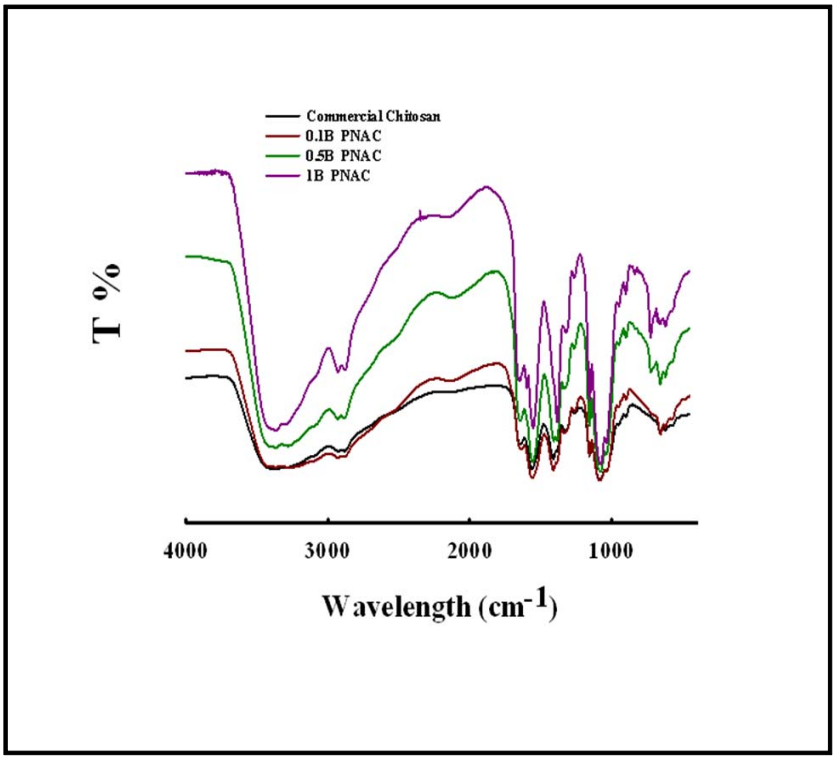

(a)

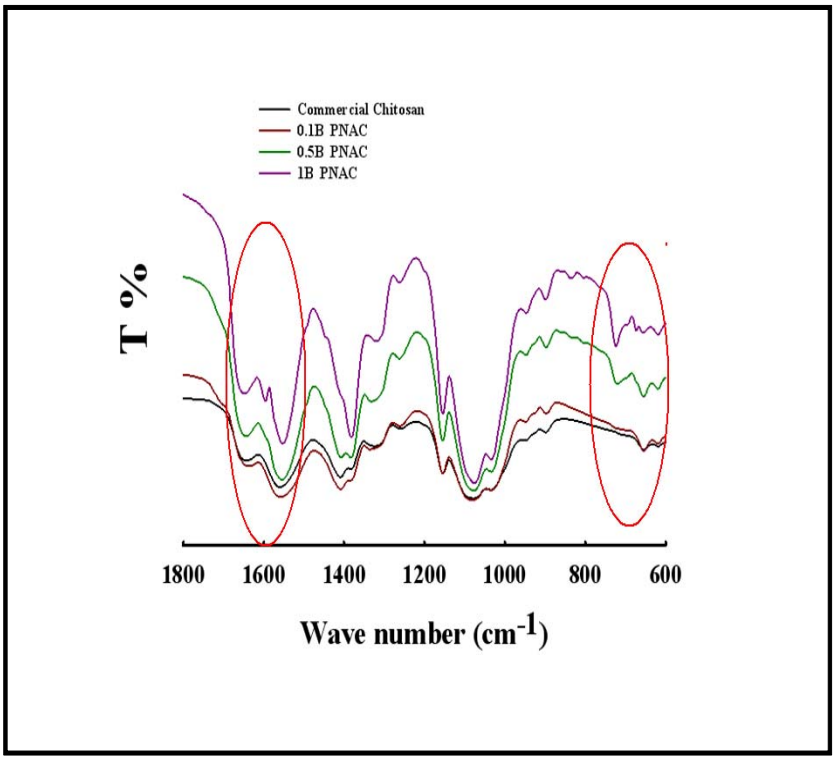

(b)

Figure 4.4. FTIR spectra of commercial chitosan and PNACs with benzoic anhydride (a) whole middle infrared region, and (b) 1800–600 cm^{-1}.

Figure 4.4.b gives the the FTIR spectra of 0.1 mol ratio benzoic anhydride modification (0.1B PNAC).0.5 mol ratio benzoic anhydride modification (0.5B PNAC), 1 mol ratio benzoic anhydride modification (1B PNAC). Amide I and amide II bands are observed as in valeric anhydride modification. The only difference is the peak around 1592 cm-1 which might be ascribed as benzene groups. Because the aromatic rings are observed around 1580 cm^{-1} especially stronger when the ring is further conjugated. The peak around 3000 cm^{-1} is considered as C-H structures in aromatic rings .In Figure 4.4 an increment in two peaks around this region is observed as the initial mol ratio of benzoic anhydride increases (California State University Stanislaus 2009).

The mono substituted benzene rings are observed in the regions of 750-750 and 660-710 cm^{-1} so the strong fingerprints in that region might be considered as aromatic rings (Wikipedia 2009).

4.2.3. X-Ray Diffraction (XRD)

The crystallinity change of chitosan by N-acylation with various acid anhydrides and initial mol ratios was determined by XRD.

Figure 4.5 and Figure 4.6 show the XRD patterns of used commercial chitosan and synthesized PNAC with various modifying agents. As it is seen from Figure 4.5 only the modification supplied by the lowest initial monomolar ratio of valeric anhydride (0.1V) was sufficient to destroy the crystalline structure of chitosan. At higher initial monomolar ratios PNACs samples like crystalline structure of commercial chitosan. The only difference was the existence of a broad X-ray diffraction intensity near $2\theta=10^{o}$ for chitosan crystalline structure which might be caused by hydrophobicity of alkyl chains. The intensity of diffractions at the $2\theta=5^{o}$ also increase as the initial mol ratio of valeric anhydride increases which might be caused by the destruction of the large number of hydrogen bonding in chitosan through the N-acylation (Choi, et al. 2007).

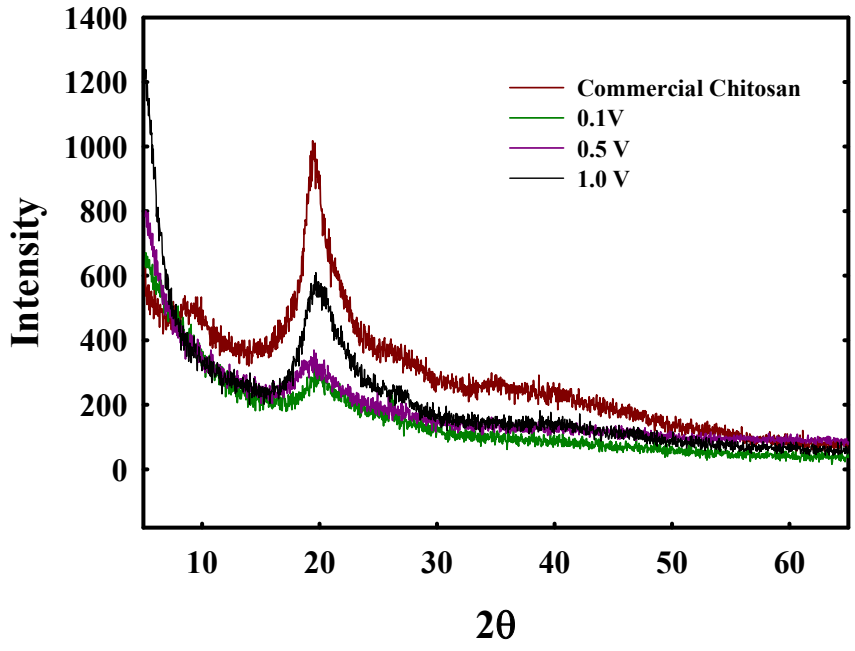

Figure 4.5. XRD pattern of PNACs with valeric anhydride at different initial mol ratio. 0.1 mol ratio valeric anhydride modification (0.1V PNAC).0.5 mol ratio valeric anhydride modification (0.5V PNAC), 1 molar ratio valeric anhydride modification (1 V PNAC).

In the case of benzoic anhydride modified PNACs (Figure 4.6), the crystallinity of chitosan was destroyed at 0.1B and 0.5B initial mol ratios. At highest initial mol ratio 1B the crystalline structure likes the commercial chitosan crystallinity. For both modification type moderately sharp intense diffraction around the $2\theta=20^{o}$.

The crystal size of samples (t) was also calculated with application of Debye Scherrer equation using XRD data (Equation (2.12)).

$$t = \frac{0.9\lambda}{\beta \cos\theta} \tag{4.5}$$

where 0.9 is the shape factor, λ is the x-ray wavelength, typically 1.542 Å, β is the line broadening at half the maximum intensity in radians, and θ is the Bragg angle which is the angle of incident beam and lattice plane which comes from the theoretical basis of X-Ray diffraction. The estimations about the crystal size of samples (t) are given in Table 4.3.

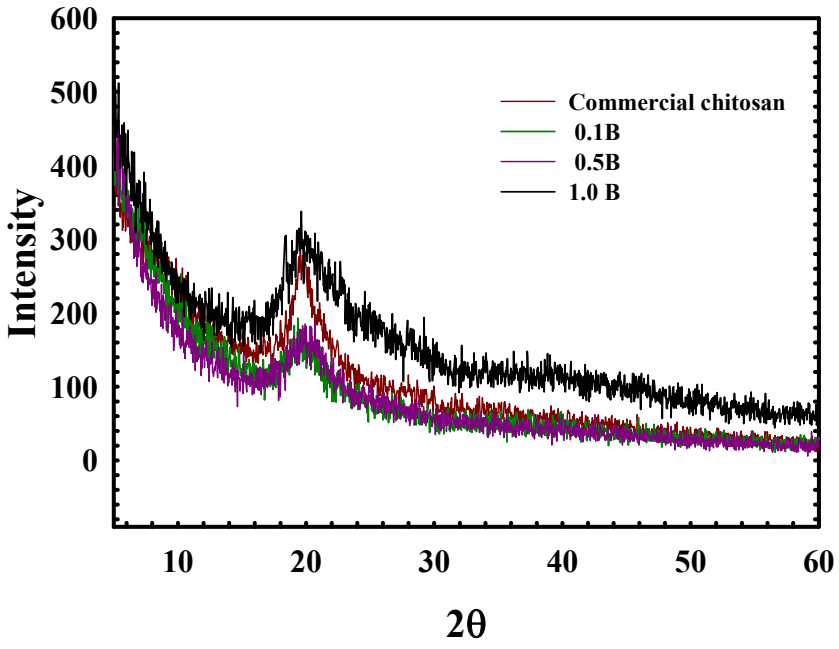

Figure 4.6. XRD pattern of PNACs with benzoic anhydride modification at different initial mol ratio. 0.1 mol ratio benzoic anhydride modification (0.1B PNAC).0.5 mol ratio benzoic anhydride modification (0.5B PNAC), 1 mol ratio benzoic anhydride modification (1 B PNAC).

Table 4.3. Estimation of crystal size of commercial chitosan and PNACs.

Sample	Crystal Size (nm)
Commercial chitosan	1.159
PNAC 0.1V	5.522
PNAC 0.5V	3.397
PNAC 1.0 V	1.982
PNAC 0.1B	2.590
PNAC 0.5B	3.087
PNAC 1.0 B	2.066

These results show that the crystal sizes of samples are affected by initial mol ratios. Such as, 0.1 V PNAC has biggest size and a decrease was observed as the initial mol ratio increases for valeric anhydride modification. However, in the case of benzoic anhydride modification, the same trend could not be observed

4.2.4. Scanning Electron Microscope (SEM) Analysis

Commercial chitosan and synthesized PNACs' morphologies were studied by SEM (Scanning Electron Microscope). The SEM images with 5 μm magnifications were shown in Figure 4.7 and Figure 4.8, respectively.

According to SEM images given in Figure 4.7 the morphology of PNACs became rougher with the lowest initial mol ratio modification (0.1V) whereas the higher initial mol ratio modifications (0.5V and 1V) make the surface smoother than the commercial chitosan surface.

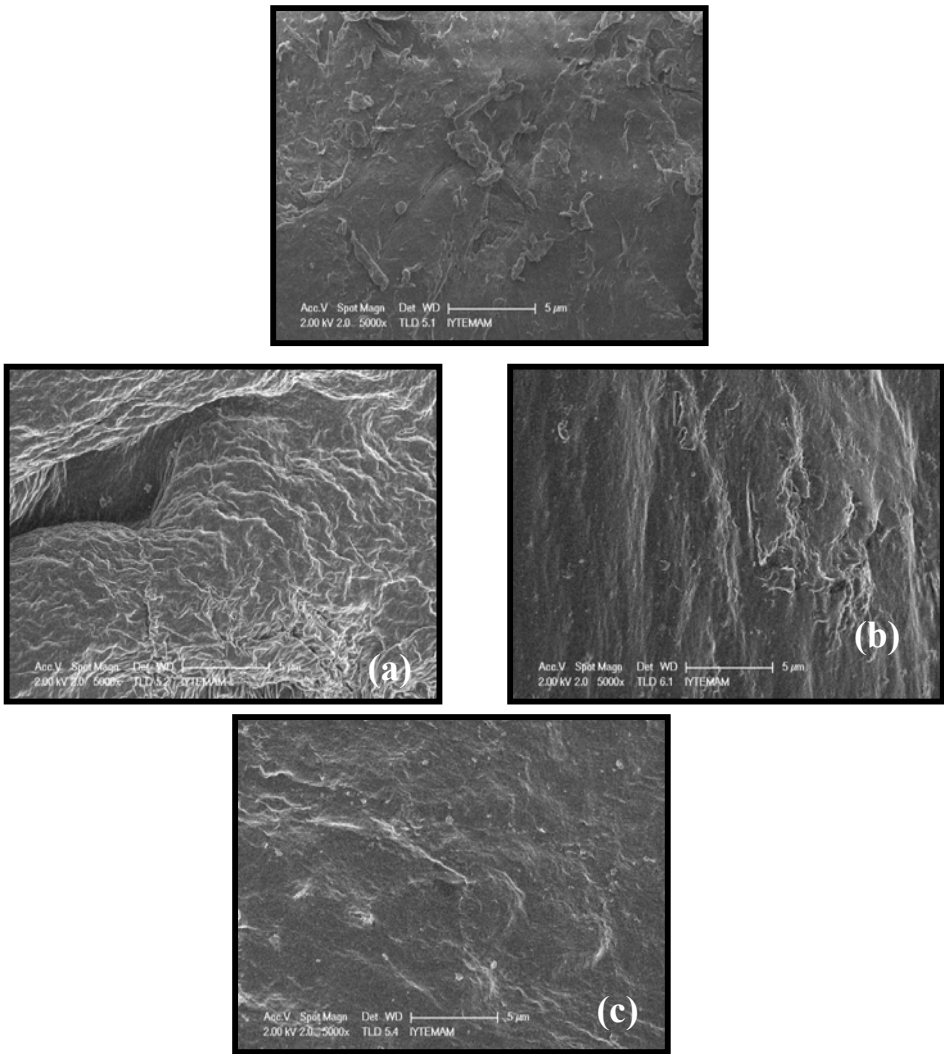

Figure 4.7. SEM image of commercial chitosan a) 0.1V b) 0.5V c) 1 V

As the initial mol ratio increases the surface pattern of PNACs modified with benzoic anhydride (0.1B, 0.5B and 1B) showed slightly rougher pattern. In this modification, irregular structures were also observed.

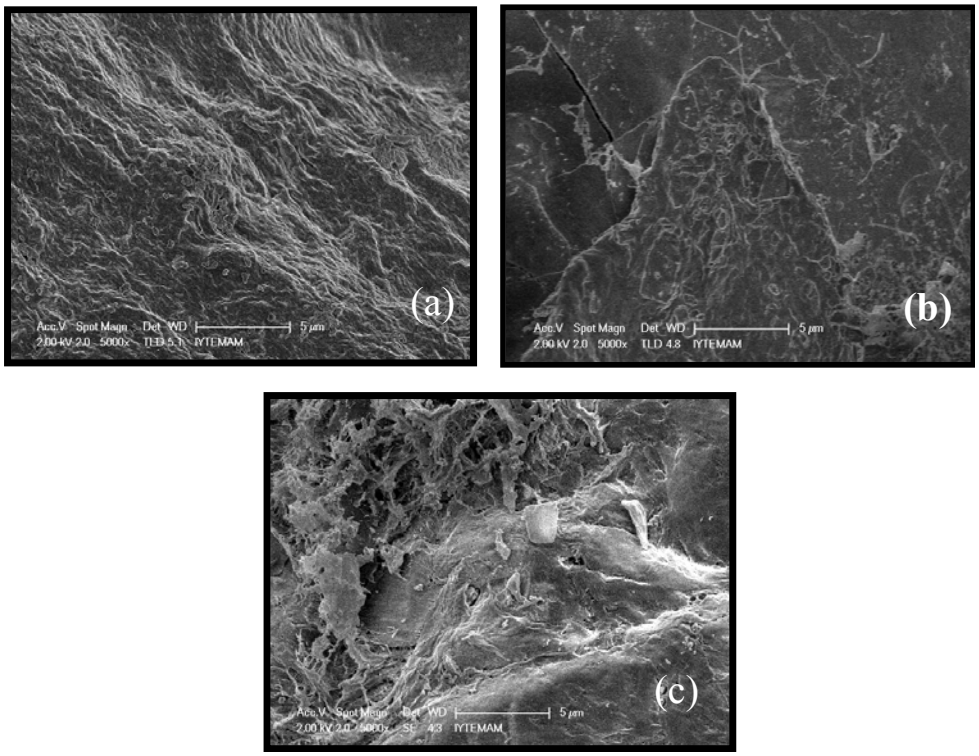

Figure 4.8. SEM image of a) 0.1B b) 0.5B c)1 B PNACs

4.2.5. Determination of Surface Activity of Partially N-acylated Chitosan

4.2.5.1. Surface and Interfacial Tension Measurements

Surface (air/water) and interfacial tension (water/oil) measurements were conducted only with low concentration of commercial chitosan and PNACs in order to provide complete solubility and prevent polymeric micelle formation. Some studies in literature, however, tested high concentrations such as 0.5 g/l^{-1} and 3.0 g/l^{-1} observed

high surface tension values which were ascribed as the polymeric micelles formation (Lee et al. 2005).These measurements usually achieved by dissolving chitosan in aqueous acetic acid solutions. Strong acids such as hydrochloric acid (HCl) aqueous solution is not preferred because HCl is observed to provide more protons, H^+, than acetic acid in the same concentration . This effect was postulated as a reason for the no difference in their surface tension values even in the case of higher concentrations of chitosan by Qun and Ajun (Qun and Ajun 2006).

In this study 5% (v/v) aqueous acetic acid solution was used in order to provide solubility utterly. When, 2% (v/v) aqueous acetic acid solution was used, the dissolution of PNACs was not complete. However, there should be a complete dissolution in order to get reproducible and correct results.

Since chitosan and PNAC were dissolved in 5% (v/v) aqueous acetic acid solution, not in water, the surface tension measurements were conducted for acetic acid solutions without chitosan first Figure 4.9 gives these values as a function of acetic acid concentration. As it is seen from the figure that the surface tension of air/acetic acid solution interface decreased significantly which makes acetic acid surface active.

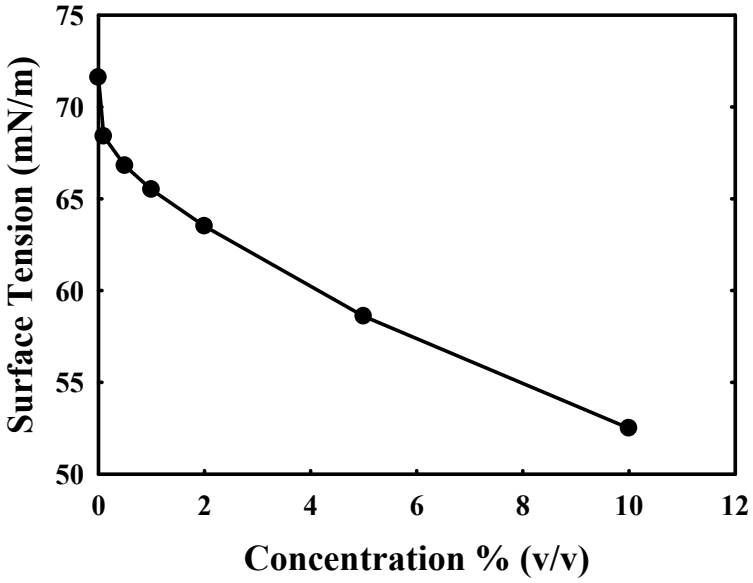

Figure 4.9. Effect of acetic acid concentration on surface tension

The hydrophobic group of acetic acid is hydrocarbon group (C_NH_M) while its hydrophilic group is a carboxyl group (COOH). The ratios of the hydrophobic group per hydrophilic group in citric acid and acetic acid are 1:2 and 1:1, respectively. Generally, the efficiency of molecule adsorption at the surface increases with the amount of the hydrophobic group and decreases with the amount of the hydrophilic group in the structure of the adsorbed molecules. Acetic acid can reduce the surface tension more effectively than citric acid since it has a lower ratio of the hydrophobic group per hydrophilic group than that of citric acid. Since citric acid has the number of hydrophilic groups two times as many as the number of hydrophobic group, citric acid has strong affinity with water and cannot be adsorbed at the surface (Permprasert and Devahastin 2005).

Table 4.4. Surface tension of PNACs at various types and concentrations.

Samples	Surface Tension (mN/m)	Interfacial Tension (mN/m)
Ultrapure water	71.6	47.3
5% (v/v) AcOH aq.sol.	58.6	31.7
0.1V		
0.01% (w/v) 0.1V	49.8	36.5
0.03 % (w/v) 0.1 V	57.3	34.7
0.5 V		
0.01% (w/v) 0.5V	48.7	37.0
0.03% (w/v) 0.5V	51.3	34.4
1 V		
0.01% (w/v) 1.0V	44.2	31.8
0.03% (w/v) 1.0 V	50.6	30.7
0.1B		
0.01% (w/v) 0.1B	48.7	36.5
0.03% (w/v) 0.1B	54.8	34.7
0.5B		
0.01% (w/v) 0.5B	46.4	33.6
0.03% (w/v) 0.5B	51.9	32.3
1B		
0.01% (w/v) 1.0 B	45.2	32.6
0.03% (w/v) 1.0 B	46.3	26.3

Surface and interfacial tension values of chitosan and PNAC in acetic acid solution were also given in Table 4.4 for the concentrations used in this study. It is seen from the table that the both chitosan and PNAC decreased the surface tension value further compared to the acetic acid; however, their effect is complex. This might be due to the possible changes in their structures when the number of these molecules increased in the system. These changes will be more possible in the case of modified chitosan molecules due to interactions between the hydrophobic sides of the molecules. The presence of hydrogen bonding due to OH groups present in the structure and electrostatic interactions due to the free NH_2 groups (if any) in the solutions of chitosan and PNACs are also expected to influence the value of surface tension.

The interfacial tension values, on the other hand, did not change much in the presence of chitosan and modified chitosan molecules.

4.2.5.2. Contact Angle Measurements

Contact angle measurements were utilized to determine the hydrophobic characteristics of commercial chitosan and synthesized PNAC. Table 4.5 and

Figure 4.10 represent the contact angle values obtained in chitosan/water/air and PNAC/water/air systems. In the case of chitosan alone, there was no angle formed. Chitosan was wettable. In the case of modified chitosan, however, the angle formed and changed between 63 and 113 degrees depending on the initial mol ratio. That is the hydrophobicity of PNACs increased as the initial mol ratio increase because of the increment in the number of hydrophobic groups, alkyl and benzene groups. As it is seen the values were higher in the presence of benzene groups in the system. This shows the success of the surface active biopolymer formation.

Table 4.5. Contact Angle Results of PNACs in Solid Disk Form**.**

Sample	Contact Angle(o)
Commercial Chitosan	0
PNAC 0.1 V	63
PNAC 0.5 V	70
PNAC 1.0 V	97
PNAC 0.1 B	72
PNAC 0.5 B	91
PNAC 1.0 B	113

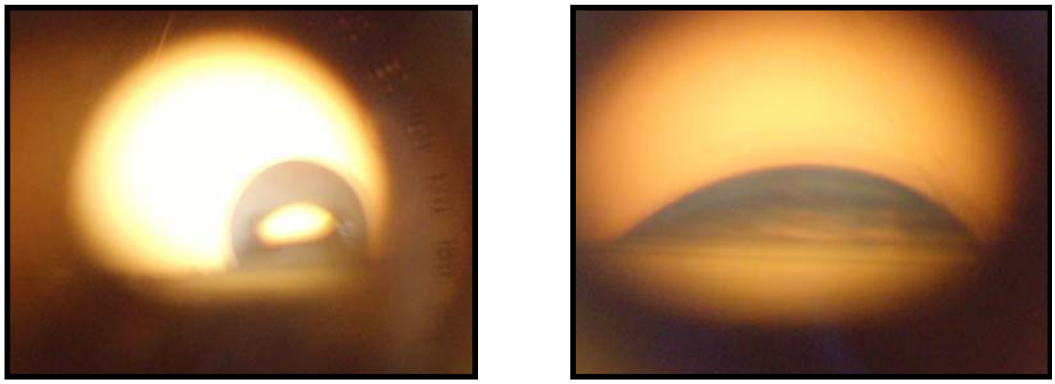

Figure 4.10**.** Photographs of water droplets on 0.1Vand 1V PNAC samples.

4.3. Use of Partially N-acylated Chitosan as an Emulsifier

4.3.1. Emulsification of Dodecane in the Absence of Chitosan

First of all, the kinetics of dodecane emulsification in the absence of chitosan was investigated. This experiment was conducted in ultrapure distilled water. The results were presented as X_{50} (median average) versus concentration plots by applying the phenomenological dispersion model discussed above (see Chapter 1 and 2).Also the breakage rate (k_b) and coalescence rate (k_c) of each prepared conditions were calculated

by using phenomenological dispersion model and given in Table 4.6 The details of the experiments will be discussed in the following paragraphs as follows.

Table 4.6. The breakage rate constants

CONDITIONS	DISPERSION RATES	
Dodacane in water	-0.3086	(between 8 and 12 minute) 6.0317
Dodacane in 2% aq.AcOH	-0.4085	(after 4 minute) -0.8323
Dodacane in 5% aq.AcOH	-0.5899	(after 16 minute) -1.8525
Chitosan in 5% aq.AcOH		
0.005% chitosan		
0.01% chitosan	-0.1971	(after 8 minutes) -0.1067
0.02% chitosan	-0.2343	(between 8-16 minutes) -9.5708e-3
0.03% chitosan	-0.3541	(after 16 minutes) -0.30513
0.1V in 5% aq.AcOH		
0.01%0.1 V	-0.187	
0.02% 0.1V	-0.3007	(after 12 minutes) -0.0891
0.03% 0.1V	-0.2147	(after 24 minutes) -0.0569
0.5V in 5% aq.AcOH		
0.005% 0.5V	-0.0888	(after 4 minutes) -0.3421
0.01%0.5 V	-0.1889	
0.02% 0.5V	-0.1708	
0.03% 0.5V	-0.2384	
1V in 5% aq.AcOH		
0.005% 1V	-0.1925	
0.01% 1 V	-0.1668	(after 16 minutes) -0.3632
0.02% 1 V	-0.1053	(after 12 minutes) -0.6707
0.03% 1V	-0.2077	
0.1B in 5% aq.AcOH		
0.005% 0.1B	-0.1563	
0.01%0.1 B	-0.1743	(after 32 minutes) -0.3443
0.02% 0.1B	-0.2083	(after 28 minutes) -0,0462
0.03% 0.1B	-0.2055	(after 20 minutes) -0.0290
0.5B in 5% aq.AcOH		
0.005% 0.5B	-0.2054	
0.01%0.5 B	-0.2334	
0.02% 0.5B	-0.2276	
0.03% 0.5B	-0.2053	
1B in 5% aq.AcOH		
0.005% 1B	-0.2248	(after 8 minute) -0.0451
0.01% 1 B	-0.2053	
0.02% 1 B	-0.1459	
0.03% 1B	-0.2336	(after 28 minutes) -0,1065

The results of dodecane emulsification in ultrapure water and in acetic acid are presented in Figure 4.11 It is seen that the size of the dodecane droplets in ultrapure water, decreased first with the breakage rate (k_b = –0.3086) and then started to increase after 8 minutes of emulsification. In the first 8 minutes, the dominant mechanism is dispersion ($k_b > k_c$), after 8 minutes of emulsification, coalescence becomes the dominant mechanism ($k_b < k_c$) and the size of dodecane droplets kept increasing with time during this experiment. Whereas 2 % and 5% (v/v) aqueous acetic acid solutions showed nearly the same effect on emulsion kinetic. In 2% (v/v) aqueous acetic acid solution breakage rate increased after first 4 minute. However, in 5% (v/v) aqueous acetic acid solution breakage rate has an increment after 16 minute. All in all, in both concentrations the dominant mechanism is dispersion ($k_b > k_c$) and have same rate trend. There is a little difference between the concentration effects of acid concentrations.

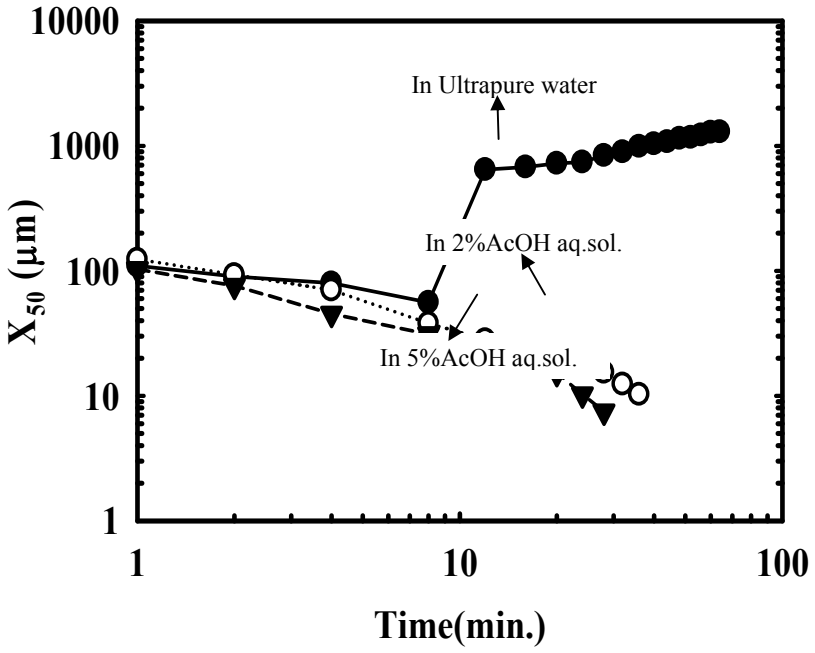

Figure 4.11. The size of dodecane droplets as a function of time in ultrapure water, 2%, 5% (v/v) acetic acid aqueous solution.

4.3.2. Emulsification of Dodecane in the Presence of Chitosan

4.3.2.1. Effect of Chitosan Concentration in 2 %(v/v) Aqueous Acetic Acid Solution

Figure 4.12 gives the effect of chitosan concentration on the kinetics of the oil emulsification when dodecane was dispersed in 2% (v/v) acetic acid aqueous solution.

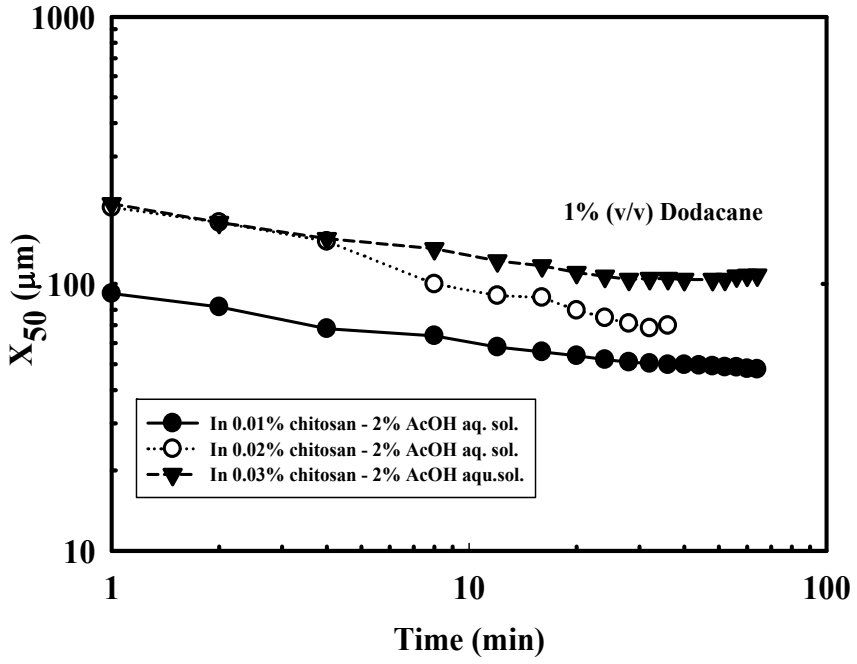

Figure 4.12**.** Change in the median droplet sizes as a function of time at different chitosan concentration in 2 % (v/v) acetic acid solution

It is seen that the rate of change of droplet size stayed constant throughout the experiment. That is the dominant mechanism in the emulsification of dodecane in the presence of chitosan is always dispersion ($k_b > k_c$). However, the both rates are not very different from each other. k_b is very small also k_b and k_c are almost equal. On the other hand for first 1 minute the droplet sizes are observed as little larger in the presence of higher chitosan concentrations.

4.3.2.2. Effect of Chitosan Concentration In 5% (v/v) Aqueous Acetic Acid Solution

Similar set of experiments were also conducted in the case 5% (v/v) acetic acid solution. Figure 4.13 illustrates the results. The effect of chitosan concentration is negligible. All the concentrations of chitosan, 0.005 % (w/v), 0.01% (w/v) and 0.02% (w/v), have the same effect on oil dispersion. The difference was observed when the concentration reaches to 0.03 % (w/v). The median droplet size became smaller when the concentration was increased which might be caused by the existence of more chitosan molecules when small droplets occur that will prevent coalescence of droplets.

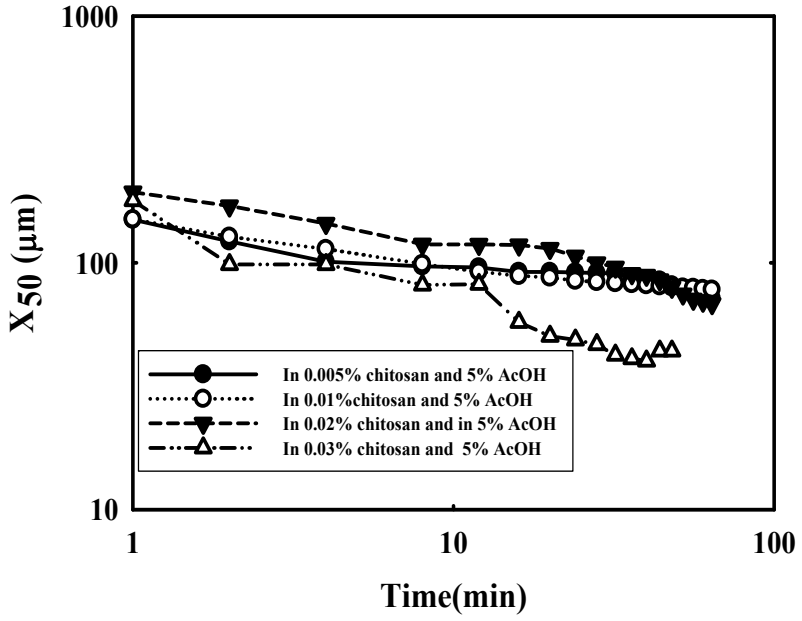

Figure 4.13. Change in the median droplet sizes as a function of time at different chitosan concentration in 5 % (v/v) acetic acid solution

4.3.3. Emulsification of Dodecane in the Presence of Chitosan Based Surface Active Polymers

In this part of the study, the effect of PNACs on the kinetics of dodecane emulsification was investigated in the presence of these polymers. The results of these studies are discussed in the following paragraphs using similar type of plots and dispersion model.

4.3.3.1. Effect of Different Type of Partially N-acylated Chitosan

The effect of PNAC, modified with different initial mol ratios of valeric anhydride, on the kinetics of dodecane emulsification was tested. In these experiments the concentrations of these polymers were kept constant. The results are presented in Figure 4.14 together with the results of initial studies (dodecane emulsification in the absence and presence of chitosan in acetic acid solution) discussed above for comparison purposes. It can be seen from the figure that the effect of initial mol ratio on the rate of breakage is negligible. The rate constants are similar for all the cases. The droplet size, on the other hand, is larger in the case of the lowest and the highest mol ratios. The general behavior of this surface active polymers are very similar in tested concentrations but the PNAC with 1 mol initial ratio of valeric anhydride shows a different trend with the increment of dispersion rate after 16 minutes.

Similar types of experiments were also conducted using benzoic anhydride to modify chitosan. The same types of results were observed. The effect of initial mol ratio on the emulsification of dodecane was negligible. This suggests that droplets are surrounded with sufficient amount of hydrophobic groups even in the case of 0.1B modification. At higher concentrations, surface active polymers may form polymeric micelles so only certain amount of hydrophobic groups (similar amount of hydrophobic groups) may reach to surfaces of droplets to decrease surface tension, increase breakage rate and therefore decrease droplet size. These results are in good agreement with the results of surface tension measurements (Table 4.4).

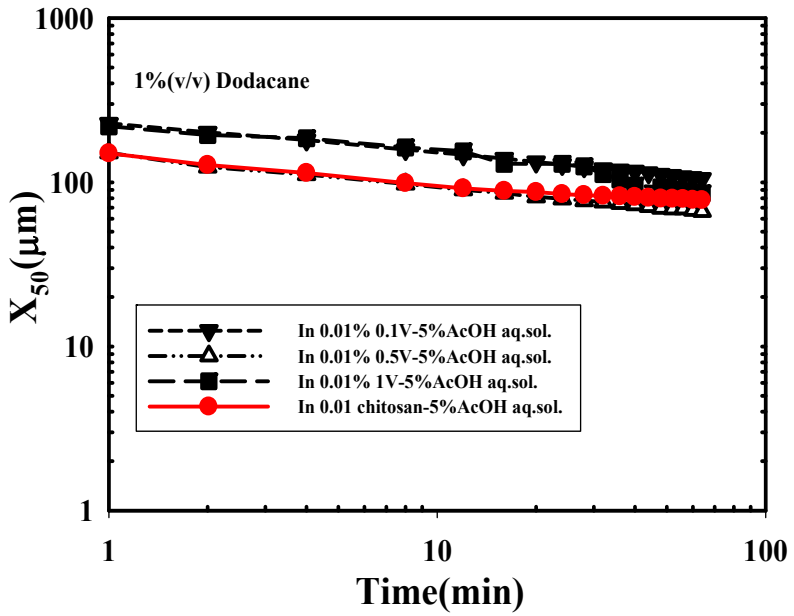

Figure 4.14. Change in the median droplet sizes as a function of time with different valeric anhydride modifications. 0.1 mol ratio valeric anhydride modification (0.1V).0.5 mol ratio valeric anhydride modification (0.5V), 1 mol ratio valeric anhydride modification (1V)

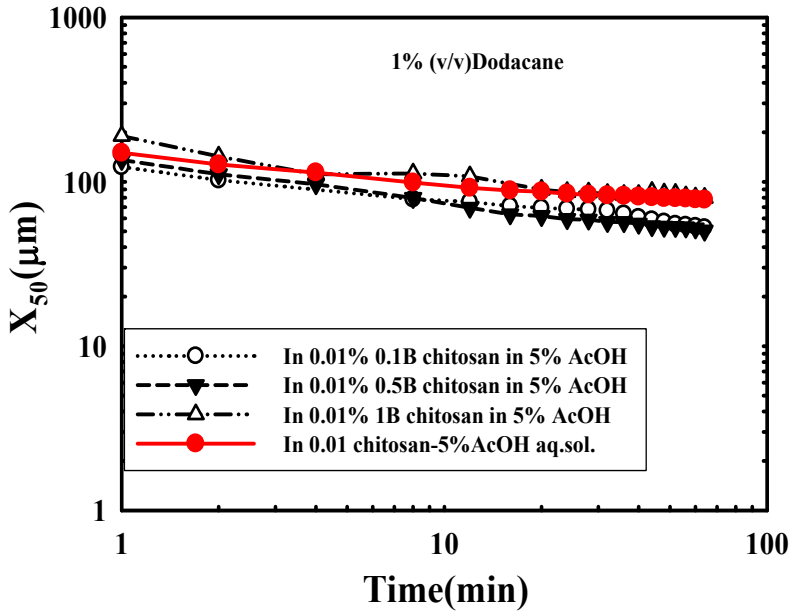

Figure 4.15. Change in the median droplet sizes as a function of time with different benzoic anhydride modifications. 0.1 mol ratio benzoic anhydride modification (0.1B).0.5 mol ratio benzoic anhydride modification (0.5B), 1 mol ratio benzoic anhydride modification (1B)

4.3.3.2. Effect of Different Type of Partially N-acylated Chitosan Concentration

4.3.3.2.1. PNAC modified with Valeric Anhydride

In this part of the study, the effect of valeric anhydride modified PNAC on the kinetics of dodecane emulsification was tested as a function of its concentration (0.01, 0.02, 0.03%) for the three initial mol ratios, 0.1, 0.5 and 1.0. The results are represented in Figure 4.16, Figure 4.17 and Figure 4.18 respectively. It is seen that the effect of polymer concentration was negligible when the initial mol ratio of acid anhydride was constant in the case of 0.5 V initial mol ratios. In case of other mol ratios the effect of concentration on the droplet size was complex.

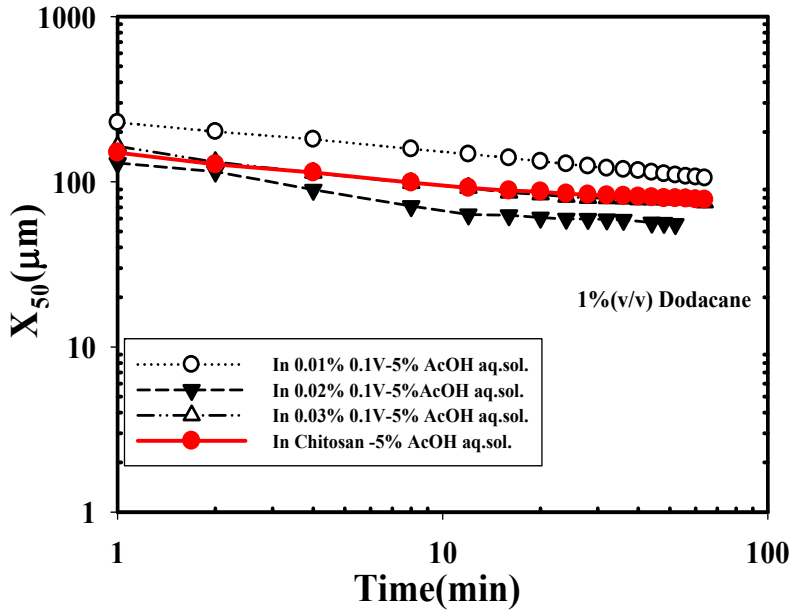

Figure 4.16. Change in the median droplet sizes as a function of time with different concentrations of 0.1 mol initial ratio valeric anhydride modification (0.1V)

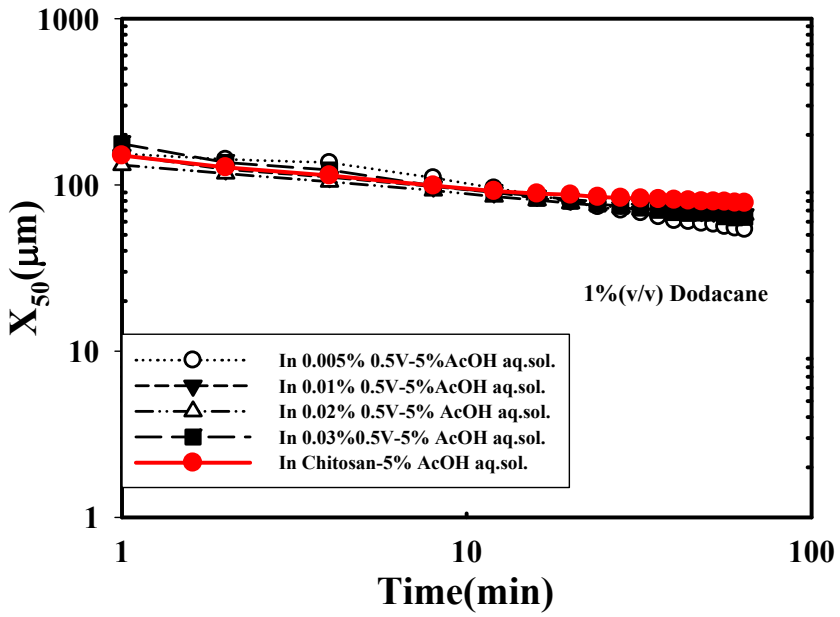

Figure 4.17. Change in the median droplet sizes as a function of time with different concentrations of 0.5 mol initial ratio valeric anhydride modification (0.5V)

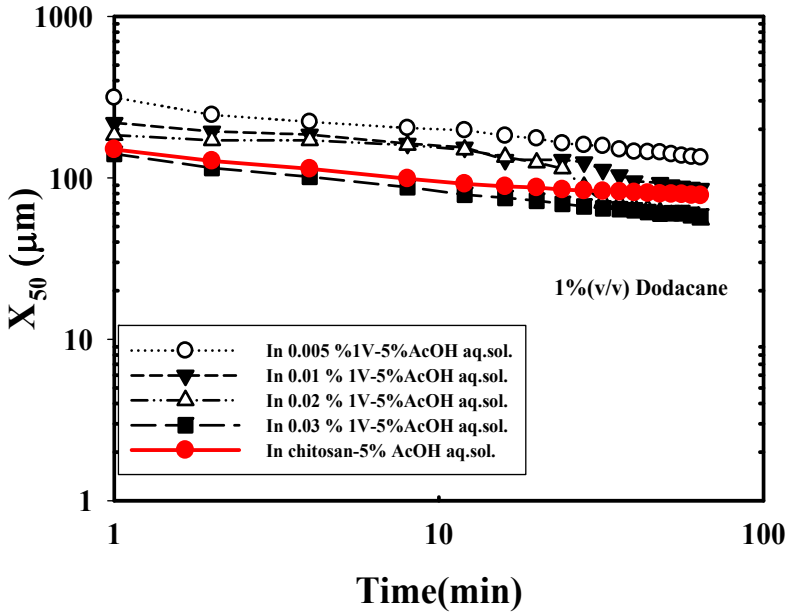

Figure 4.18. Change in the median droplet sizes as a function of time with different concentrations of 1 mol initial ratio valeric anhydride modification (1V).

4.3.3.2.2. PNACs with Benzoic Anhydride

In this part of the study, the effect of benzoic anhydride modified PNAC on the kinetics of dodecane emulsification was tested as a function of its concentration for the three initial mol ratios, 0.1, 0.5 and 1.0 . The results are represented in Figure 4.19, Figure 4.20, and Figure 4.21, respectively. It is seen that the effect of polymer concentration was negligible when the initial mol ratio of acid anhydride was constant. The same trend was also observed for the three initial mol ratios tested.

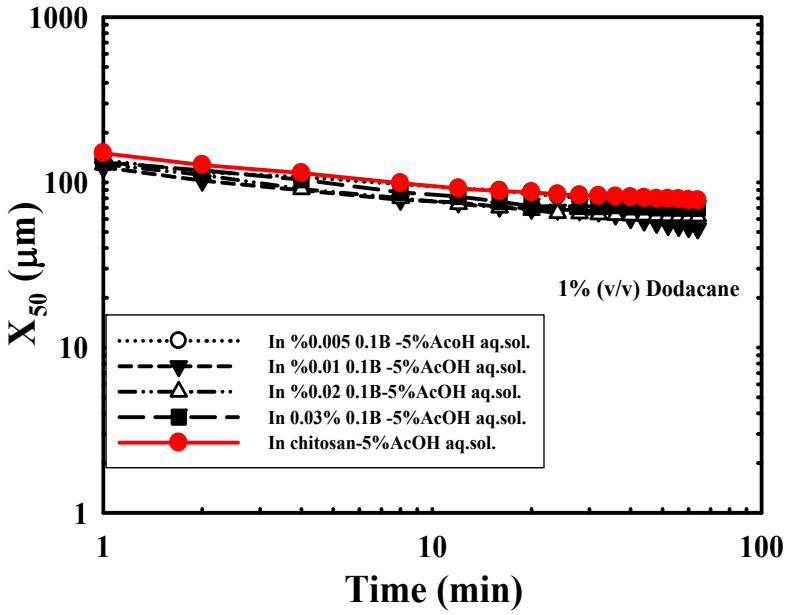

Figure 4.19. Change in the median droplet sizes as a function of time with different concentrations of 0.1 mol initial ratio benzoic anhydride modification (0.1 B)

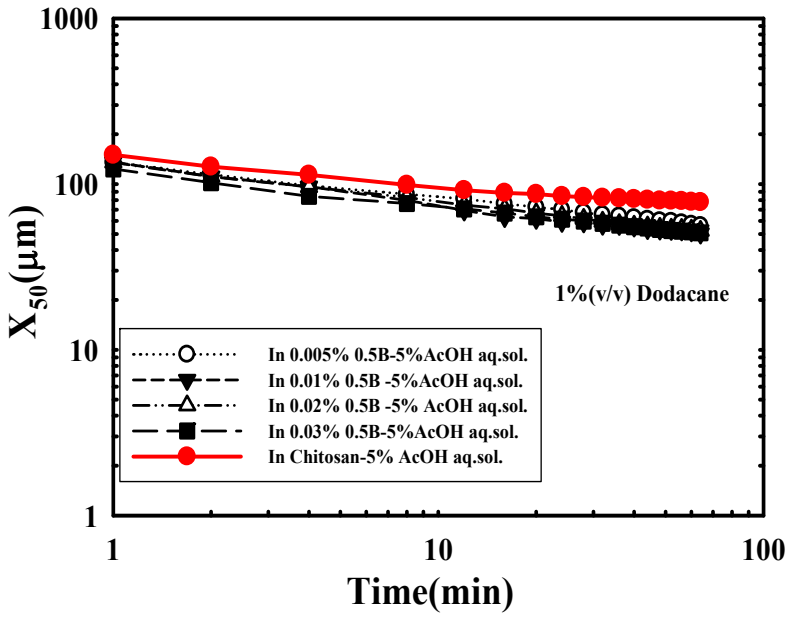

Figure 4.20. Change in the median droplet sizes as a function of time with different concentrations of 0.5 mol initial ratio benzoic anhydride modification (0.5B)

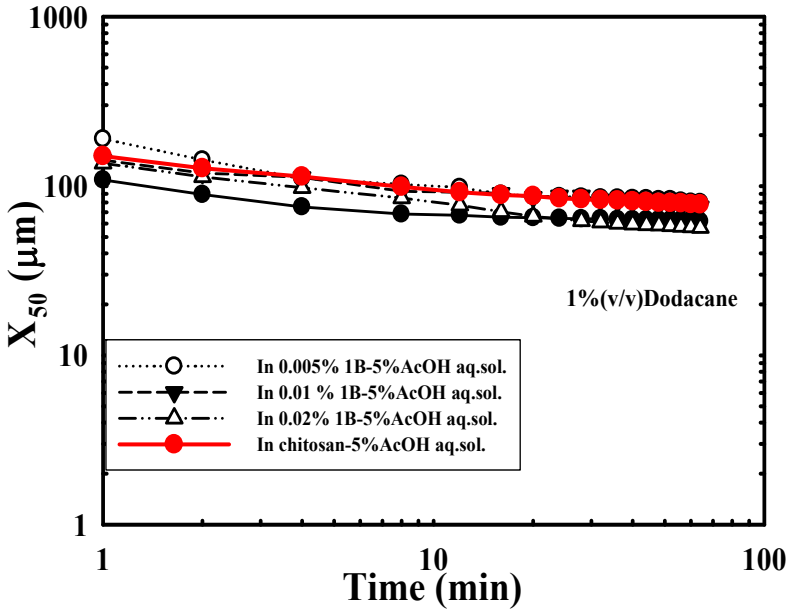

Figure 4.21. Change in the median droplet sizes as a function of time with different concentrations of 1 mol initial ratio benzoic anhydride modification (1 B).

4.4. Discussion

Emulsions are usually achieved by applying mechanical energy in the form of agitation which deforms the interface between the oil droplets and the continuous phase to such an extent that smaller daughter droplets form as discussed in Chapter 2 in detail. Change in the size distribution of oil droplets in an agitated vessel with time depends mainly on two sub-processes: *dispersion* and *coalescence*. Either of these sub-processes may dominate depending on the agitator speed, oil concentration and the additives present in the system. Surface active additives, i.e. chitosan and chitosan based bio polymers in this study, are expected to affect these sub processes by influencing:

- *the oil/water interfacial tension*: Surface active additives are expected to adsorb at oil/water interface and expected to decrease the interfacial tension. A reduction in the restoring surface tension force against deformative stresses such as those induced by eddies in turbulent mixing promotes the dispersion of oil. In addition, oil droplets dispersed in water may develop a surface charge depending on solution chemistry (Adamson 1990; Hiemenz 1986) which leads to development of an electrical double layer. The presence of such layer affects the interaction of two oil droplets electrostatically. Adsorbed species are expected to alter the degree of interaction between the droplets by influencing the profile of the double layer.
- *film drainage*: Coalescence of two oil droplets is only possible if the water film between the two can drain away within the duration of contact. The presence of free hydrated surface active molecules or micelles within the water film increases the energy required for drainage (Nikolov and Wasan, 1989), hence reducing its rate. This results in an increase in the stability (dispersion) of the system.
- *steric interactions*: Depending on the type of surface active molecule and the adsorption mechanism, molecules adsorbed at the oil/water interface may have hydrated sections extending outwards from each droplet surface. When two such droplets approach each other, the extended regions of the surface active molecules physically interact, preventing further approach for successful coalescence (steric stabilization).

Therefore, the dominant sub-process that determines the outcome of the emulsification process will be the result of all these molecular events going on in the system. When the results of all the experiments conducted in this study evaluated together, it can be concluded that the kinetics of emulsification of oil did not change much with the addition of chitosan and chitosan based bio-polymers. The rate constant of dispersion was almost similar for all these cases. However, in the case of chitosan the droplet size obtained after 1 minute stayed almost constant and did not increased after 8 minutes due to coalescence as in the case of water only. That is the breakage rate is almost equal to coalescence rate. This might be explained by the insignificant changes in interfacial tension (oil/water) values. This implies the presence of molecules in the continuous phase rather than the oil/water interface. The presence of these molecules prevents coalescence of droplets due to increase in the energy needed for film drainage. The effect of chitosan derivatives, on the other hand, was not much different than the chitosan itself even though they were proven to be more hydrophobic (see contact angle studies). This might be due to the change in their molecular configurations when they become more hydrophobic. Therefore, the bigger and heavier structures formed may have problems in terms of diffusion and surface activity in the system. This might be the reason that they are not more effective in emulsification of dodecane compare to the more hydrophilic chitosan. However, the stability (durability in time without application of mechanical energy) of these emulsion systems in the presence of these molecules at high concentrations of oil needs to be studied in detail. This may be the subject of another study in the future.

CHAPTER 5

CONCLUSIONS

In this study, biopolymeric emulsifiers (partially N-acylated chitosan) were produced and used in oil/water emulsion systems. For this purpose, chitosan was used as a raw material due to its high biocompatibility. The produced emulsifiers were characterized by the following methods: Elemental Analysis, IR Spectroscopy, degree of substitution analysis, X-Ray Diffraction (XRD), Scanning Electron Microscopy (SEM), Surface tension, O/W interfacial tension and contact angle measurements.

To study the effect of these biopolymeric emulsifiers on the kinetics of oil dispersion in water, a designed set-up was used to carry out *in-situ* size distribution measurements as a function of time by using light scattering. This set-up was consisted of a standard vessel with four baffles and turbine type stirrer. The parameters such as; oil concentration, chitosan concentration, modified chitosan concentration and type of chitosan modification (The type of substituted groups), were investigated to determine the effects on the kinetics of dispersion of oil in water. A phenomenological dispersion model was used to evaluate the size distribution data obtained in this study.

The following specific conclusions were obtained.

- The chitosan based bio-polymers were produced and shown (using XRD, FTIR, SEM, Elemental analysis etc.) to have properties sufficient to be used as an emulsifier.
- The surface tension values were found to decrease from 71 mN/m down to 40-50 mN/m in the presence of chitosan and chitosan based bio-polymers.
- The interfacial tension values obtained in the presence of chitosan and chitosan based bio-polymers were found to be similar to each other.
- Contact angle values increased significantly in the case of chitosan based biopolymers depending on their concentration and initial mol ratios significantly.
- The kinetics of emulsification of oil did not change much with the addition of chitosan and chitosan based bio-polymers. The rate constant of dispersion was almost similar for all these cases. However, in the case of chitosan and

its derivatives the droplet size obtained after 1 minute stayed almost constant and did not increased after 8 minutes due to coalescence as in the case of water only.

REFERENCES

Abismaïl, B., Canselier J. P., Wilhelm, A. M., Delmas H.,Gourdon C. 2000. Emulsification processes: on-line study by multiple lights scattering measurements .*Ultrasonics Sonochemistry 7*: *187-192*.

Akoh, C.C., Min D.B., 2008. Food lipids: chemistry, nutrition, and biotechnology, 3 rd edition, CRC Press,Taylor &Francis Group,USA.

Amass, W., Amass, A., Tighe B. 1998 .A Review of Biodegradable Polymers: Uses, Current Developments in the Synthesis and Characterization of Biodegradable Polyesters, Blends of Biodegradable Polymers and Recent Advances in Biodegradation Studies. *Polymer International 47* : *89-144* .

Beckham Coulter. http://www.beckman.com/coultercounter/product_multisizer3.jsp (accessed October 10, 2009)

Bratskaya, S., Avramenko, V., Schwarz, S., Philippova, I. 2006. Enhanced flocculation of oil-in-water emulsions by hydrophobically modified chitosan derivatives. *Colloids and Surfaces A: Physicochem. Eng. Aspects 275: 168–176.*

California State University Stanislaus.
http://www.chem.csustan.edu/Tutorials/INFRARED.HTM (accessed November 9, 2009)

Choi, C.Y., Kim S.B., Pak, P.K., Yoo, D., Chung, Y.S. 2007. Effect of N-acylation on structure and properties of chitosan fibers. *Carbohydrate Polymers 68* :*122-127.*

Dallwoo-Chitosan Corparation.
http:// members,tripıd.com/~Dalwoo/structure.html. (accessed October 20, 2009)

Dickinson, E. 2003. Hydrocolloids at interfaces and the influence on the properties of dispersed systems. *Food Hydrocolloids 17*: *25-39*.

Dutta, K.P., Dutta, J.,Tripathi, V.S. 2004. Chitin and chitosan: Chemistry,properties and applications. *Journal of Scientific & Industrial Research.63*:*20-31*.

Egger, H., McGrath, K.M. 2006. Aging of oil-in-water emulsions: The role of the oil *Journal of Colloid and interface Science 299*:*890-899*.

Friberg S.E.,Larsson, K.,Sjöblom, 2004. Food Emulsion, 4th edition, Marcel Dekker, Inc., USA.

Hench, L.L. 1998, Biomaterials: aforecast for the future. *Biomaterials 19*:*1419-1423*.

Hiemenz, P.C.,1985. Principles of Colloid and Surface Chemistry, Dekker, Newyork.

Hırano, S., Tsuneyasu, S., Kondo, Y. 1980.Heterogeneous Distribution of Amino Groups in Partially N-acylated Derivatives of Chitosan. *Agric.Biol.Chem.45:1335-1339*.

Holland, F.A., Chapman, F.S. (1966) Liquid mixing and processing in Stirred Tanks, Reinhold, Newyork

Illum L. 1998. Chitosan and its use as pharmaceutical excipient.Pharmaceutical Researh 15:1326-1331.

Jumaa, M., Muller,B.W. 1999. Physicochemical properties of chitosan-lipid emulsions and their stability during the autoclaving process. International Journal of Pharmaceutics 183 :175–184.

Kasaaı, M.R.,2007. Calculation of Mark-Houwink-Sakurada (MHS) equation viscometric constants for chitosan in any solvent-temperature system using experimental reported viscometric constants data. *Carbohydrate Polymers 68*:*477-488.*

Kinsella, J.E., 1990. Advances in Food and Nutrition Research, Volume 34, Academic Pres Inc., USA.

Kissa, E. 1999. Dispersions Characterization, Testing, and Measurement.Surfactant series volume 84 , Marcel Dekker, Inc., USA.

Koshy, A., Das, T.R., Kumar R. 1988. Effect of surfactant on drop breakage in turbulent liquid dispersions. *Chem. Eng. Sci. 43: 649.*

KRUSS.http://kruss.de/en/theory/measurements/surface-tension/ringmethod.html. (accessedNovember 10, 2009)

KSV. http://www.ksvinc.com/contact_angle.htm (accessed November 10, 2009)

Kumar Anal, A., Tobiassen, A., Flanagan J. 2008. Preparation and characterization of nanoparticles formed by chitosan–caseinate interactions . *SinghColloids and Surfaces B: Biointerfaces 64* :*104–110*.

Leal-Calderon, F., Schmitt, V., Bibette J. 2007. Emulsion Science: Basic Principles, 2nd edition, Springer Science and Business Media, USA.

Lee M.Y., Hong K.J., Kajiuchi, T.,. Yang, J.-W. 2005. Synthesis of chitosan-based polymeric surfactants and their adsorption properties for heavy metals and fatty acid. International Journal of Biological Macromolecules 36 : 152-158.

Lee, K.Y., Ha, W.S., Park W. H. 1995. Blood compability and biodegradability of partially N-acylated chitosan derivatives. *Biomaterial 16*: *1211-1216*.

Li, Q., Weng, S., Wu, J., and Zhou, N. 1998. Comparative Study on Structure of Solubilized Water in Reversed Micelles. 1 FT-IR Spectroscopic Evidence of

Water/AOT/*n*-Heptane and Water/NaDEHP/*n*-Heptane Systems *J. Phys. Chem. B* , *102*: 3168-3174.

Ligisetty J.S.,Das,R.,Gandhi, K.S. 1986. Breakage of Viscous and Non-Newtonian Drops in Siterred dispersions. *Chem. Eng. Sci. 41: 65.*

MCClement, D.J. 1999.Food Emulsions Principles, Practices and Techniques, CRC Press LLC, USA.

MCClement, D.J. 2005. Food Emulsions Principles, Practices and Techniques, 2nd edition Contemporary Food Science Series, CRC Press, USA.

Narsimhan, G., Ramkrishna , D.,and Guta J.P. 1980. Analysis of droplet size distribution in lean liquid-liquid dispersions. *AIchE Journal 26*:*99*.

Nikolov, A.D., and Wasan, D.T. 1989. Ordered micelle structuring in thin films formed from anionic surfactant solutions. *J.Colloid Interface Science 133*:*1*.

Particle and Surface Sciences.
http://www.pss.aus.net/products/micromeritics/equip_particle_size (accessed October 13, 2009)

Permprasert, J., Devahastin, S., 2005. Evaluation of the effects of some additives and pH on surface tension of aqueous solutions using a drop-weight method. *Journal of Food Engineering 70*:*219–226*.

Peter, M.G. 1995. Applications and environmental aspects of chitin and chitosan. *Journal Macromolecular science, Pure and applied Chemistry 32*: *629-640*.

Polat, H., Polat, M., Chander, S. 1999. Kinetics of oil dispersion in the absence and presence of block copolymers. *AIChE Journal 45*:*1866-1874*.

Pons, R. 2000. Polymeric surfactants as emulsion stabilizers. *Polymeric Surfactants (Surfactant Science Series)*, *409-422*.

Qun, G., Ajun, W. 2006. Effects of molecular weight, degree of acetylation and ionic strength on surface tension of chitosan in dilute solution. *Carbohydrate Polymers 64*:*29-36*.

Ramos V.M., Rodriguez N.M., Rodriguez M.S., Heras A., Agullo E., *2003.* Modified chitosan carrying phosphonic and alkyl groups. *Carbohydrate Polymers 51*:*425-429*.

Rodrıguez, M.S., Albertengo, L.A., Agullo, E.,2002. Emulsification capacity of chitosan. Carbohydrate polymers 48 : 271-276.

Shinnar, R. 1961. On the behavior of liquid dispersions in mixing vessels. *Fluid Mech. 10:259.*

Sigma Aldrich. www.sigmaaldrich.com (accessed November 5, 2009)

The Simple TEM and SEM http://commons.wikimedia.org/wiki/File: SimpleSEMandTEM.jpg (accessed October 10, 2009)

Sprow, F.B. 1967.Distribution of droplets size in turbelent flow. *AIChE Journal 8: 471*.

Swarbrick, J., Boylan, J.,2002. Encyclopedia of Pharmaceutical Technology; 2nd edition, Volume 3, Mercel Dekker Inc.,USA.

Tadros, T.F., Vandamme, A., Levecke, B., Booten, K., Stevens, C.V. 2004. Stabilization of emulsions using polymeric surfactants based on inulin. *Advances in Colloid and Interface Science 108 –109*: *207–226*.

Tatterson, G.B. 1991.Fluid Mixing and Gas Dispersion in Agitated Tanks, McGraw-Hill, Newyork .

The Tyndal Effect. http://www.chm.bris.ac.uk/webprojects2002/pdavies/Tyndall.html (accessed October 10, 2009)

Tien, C.L., Lacroix, M., Ispas-Szabo, P. Mateescu, M. A. 2003. N-acylated chitosan: hydrophobic matrices for controlled drug release. *Journal of Controlled Realease 93* :*1-13*.

Tolaimate, A., Desbrieres, J., Rhazi, M., Alagui, A., Vincendon, M., Vottero, P. 2000. On the influence of deacetylation process on the physicochemical characteristics of chitosan from squid chitin. *Polymer 41*: *2463-246.*

Tsaıh, L.M., Chen R.H.,1999. Molecular Weight Determination of 83% Degree of Decetylation Chitosan with Non-Gaussian and Wide Range Distribution by High-Performance Size Exclusion Chromatography and Capillary Viscometry. *Journal of Applied Polymer Science 71*:*1905-1913*.

University of Oslo. http://folk.uio.no/anderne/research.html) (accessed October 11, 2009)

Walstra, P.1983. Formation of emulsions . Encyclopedia of Emulsion Technology, Vol.1 , Dekker, Newyork

Wang W., Bo S., Li S., and Qin W. 1991.Determination of Mark-Houwink equation for chitosans with different degrees of deacetylation. *International Journal Biological Macromolecules 13*: *281-285*.

Wikipedia. http: // en.wikipedia.org / wiki/ Monoglyceride (accessed October 10, 2009)

Wikipedia.http: // en.wikipedia.org / wiki/ Lecithin (accessed October 10, 2009)

Wikipedia. http://en.wikipedia.org/wiki/Infrared_spectroscopy_correlation_table (accessed November 9, 2009)

Williams, D.H., Fleming, I. 1987. Spectroscopic Methods in Organic Chemistry McGraw-Hill, California .